Protolith age and deformation history of the Big Salmon Complex, relicts of a Paleozoic continental arc in northern British Columbia[1]

Mitchell G. Mihalynuk
British Columbia Ministry of Energy and Mines, PO Box 9333 Stn Prov Govt,
Victoria, BC, Canada, V8W 9N3; Mitch.Mihalynuk@gov.bc.ca

Richard M. Friedman
Department of Earth and Ocean Sciences, University of British Columbia,
Vancouver, BC, Canada, V6T 1Z4

Fionnuala A.M. Devine[2]
Department of Earth Sciences, Carleton University, Ottawa, ON, Canada, K1S 5B6

Larry M. Heaman
Department of Earth and Atmospheric Sciences, University of Alberta, Edmonton, AB, Canada, T6G 2E3

Mihalynuk, M.G., Friedman, R.M., Devine, F. and Heaman, L.M., 2006, Protolith age and deformation history of the Big Salmon complex, relicts of a Paleozoic continental arc in northern British Columbia, in Colpron, M. and Nelson, J.L., eds., Paleozoic Evolution and Metallogeny of Pericratonic Terranes at the Ancient Pacific Margin of North America, Canadian and Alaskan Cordillera: Geological Association of Canada, Special Paper 45, p.????

Abstract

The Big Salmon Complex is a belt of polydeformed sedimentary and submarine volcanic rocks that extends from northwestern British Columbia into southern Yukon. It includes newly discovered volcanogenic massive sulphide (VMS) mineralization and shares age and lithologic characteristics with the Finlayson Lake VMS district. A distinctive marker succession, the Jennings marker, is affected by four phases of deformation. Determination of protolith and deformation ages employing the U-Pb zircon technique is complicated by inheritance and lead loss. Oldest parts of the Jennings marker are apparently intruded by a polyphase granitoid interpreted to be as old as ca. 362 Ma. Interbedded and structurally underlying quartz-rich strata are intruded by a ca. 353 Ma quartz porphyry intrusion. The marker is overlain by heterolithic strata including ca. 325 Ma tuffaceous layers in limestone.

Evidence of the oldest deformation, D_1, is preserved only locally as relicts of amphibolite grade porphyroblasts. D_1 is correlated tentatively with Antler orogeny deformation that preceded opening of the Slide Mountain basin. D_1 deforma-

[1]*Data Repository items* Mihalynuk_Appendix1.pdf *(Appendix 1) and* Mihalynuk_DR1.pdf *(Figures DR1 and DR2) are available on the CD-ROM in pocket.*

[2]*Present address: Devine – 4120 Shasheen Road, Nelson, B.C. V1L 6X1.*

tion postdated the Jennings marker and the ca. 362 Ma and 353 Ma granitoid units, and predated a ca. 331 Ma intrusion that cuts D_1 fabrics. D_2 is the youngest regional transposition fabric. Its age is constrained to between ca. 325 and ca. 198 Ma; it may be related to a Late Permian collisional event that is well represented in central Yukon-Tanana terrane. D_3, the youngest regional deformation event, is characterized by large-scale, recumbent closures north of the Simpson Peak batholith and northeast-verging folds that involved Triassic strata and ca. 198 Ma intrusions. D_3 fabrics are cut by late syn- to post-kinematic phases of the ca. 185 Ma Simpson Peak batholith, and are coeval with a profound Jurassic (ca. 185 Ma) lead-loss event. D_3 is correlated with rapid uplift of parts of Yukon-Tanana terrane during early collision with the northern continental margin.

Deformational events younger than D_3 probably were related to motion on the crustal-scale Teslin fault that marks the western limit of the Big Salmon Complex. These include the development of D_4 kink folds and ductile shear fabrics affecting the 57 Ma Charlie Cole pluton. Such young ductile shear fabrics are not recognized in older rocks; a cautionary reminder that strain tends to concentrate in weak units, such as cooling plutons, and need not be regionally represented.

Résumé

Le complexe de Big Salmon est une bande de roches sédimentaires et volcaniques sous-marines polydéformées qui va du nord-ouest de la Colombie-Britannique jusqu'au sud du Yukon. Il comprend une zone minéralisée de sulfures massifs volcanogéniques (SMV), découvertes récemment, dont l'âge et les caractéristiques lithologiques ressemblent à ceux du district de SMV de Finlayson Lake. Une succession distinctive, le marqueur Jennings, a subi quatre phases de déformation. La détermination du protolithe et des âges de déformation à partir de techniques de datation U-Pb sur zircon est entravée par l'effet de phénomènes d'héritage et de perte de plomb. Les parties les plus anciennes du marqueur Jennings semblent avoir été recoupées par plusieurs phases d'un granitoïde d'un âge aussi ancien que 362 Ma. Un porphyre quartzifère a recoupé, et s'est interstratifié à des strates riches en grains de quartz structuralement susjacentes, il y a environ 353 Ma. La succession marqueur est surmontée par des strates hétérolithiques, dont des couches tufacées d'environ 325 Ma dans un calcaire.

On ne retrouve que localement des preuves de la plus ancienne phase de déformation, Di, sous forme de reliquats de porphyroblastes au faciès des amphibolites. On considère que la phase Di correspond à la déformation de l'orogenèse de Antler qui a précédé l'ouverture du bassin de Slide Mountain. La déformation de D_1 est survenue après la mise en place du marqueur Jennings et des unités de granitoïdes de 362 Ma et de 353 Ma, mais il a précédé l'intrusion de 331 Ma qui recoupe la fabrique D_1. D_2 correspond à la plus récente fabrique régionale de transposition. L'âge de cette phase se situe approximativement entre 325 Ma et 198 Ma; elle pourrait avoir un lien avec l'événement collisionnel du Permien supérieur qui est bien représenté dans le terrane de Yukon-Tanana. D_3, la déformation régionale la plus jeune, est caractérisée par des fermetures renversées de grandes amplitudes au nord du batholite de Simpson Peak, et par des plis de vergence nord-est de strates triasiques et d'intrusions d'environ 198 Ma. La fabrique D_3 est recoupées par des phases tardives syn- et post-cinématiques datant d'environ 185 Ma du batholite de Simpson Peak, et sont contemporaines d'un événement jurassique (environ 185 Ma) de perte de plomb d'une grande portée. La phase D^3 correspond au soulèvement rapide de certaines parties du terrane de Yukon-Tanana au début de la collision avec la marge continentale nord-américaine.

Les événements de déformation plus jeunes que D_3 sont probablement reliés à des déplacements d'ordre crustal le long de la faille de Teslin qui marque la limite ouest du complexe de Big Salmon. Ces derniers événements incluent le développement de plis en chevron et d'une fabrique de cisaillement ductile D4 affectant le pluton de 57 Ma de Charlie Cole. Une telle fabrique de cisaillement ductile ne se retrouve pas dans les roches plus anciennes – un rappel que les effets de la déformation sont les plus évidents sur les unités les plus malléables, comme les plutons en cours de solidification, et que ces effets pourraient ne pas être présents régionalement.

PAGE PROOFS

INTRODUCTION

Polydeformed volcanic arc strata of the Big Salmon Complex extend more than 200 km from northwestern British Columbia into southern Yukon and are now included as part of the Finlayson and Klinkit assemblages of the Yukon-Tanana terrane (Fig. 1; Colpron *et al.*, this volume-a). Historically, different parts of the Big Salmon Complex have been assigned various tectonic affiliations, but field studies conducted under the Ancient Pacific Margin NATMAP (National Mapping Program; see Mihalynuk *et al.*, 2000a, 2001a, b, and geological summary on Fig. 2; also Roots *et al.*, this volume) have helped to repatriate portions of the Big Salmon Complex that were formerly orphaned by provincial borders and various terrane definitions. Rejoined to the belt of metamorphosed miogeoclinal and superposed arc rocks to which they belong, they inherit a share of the potential

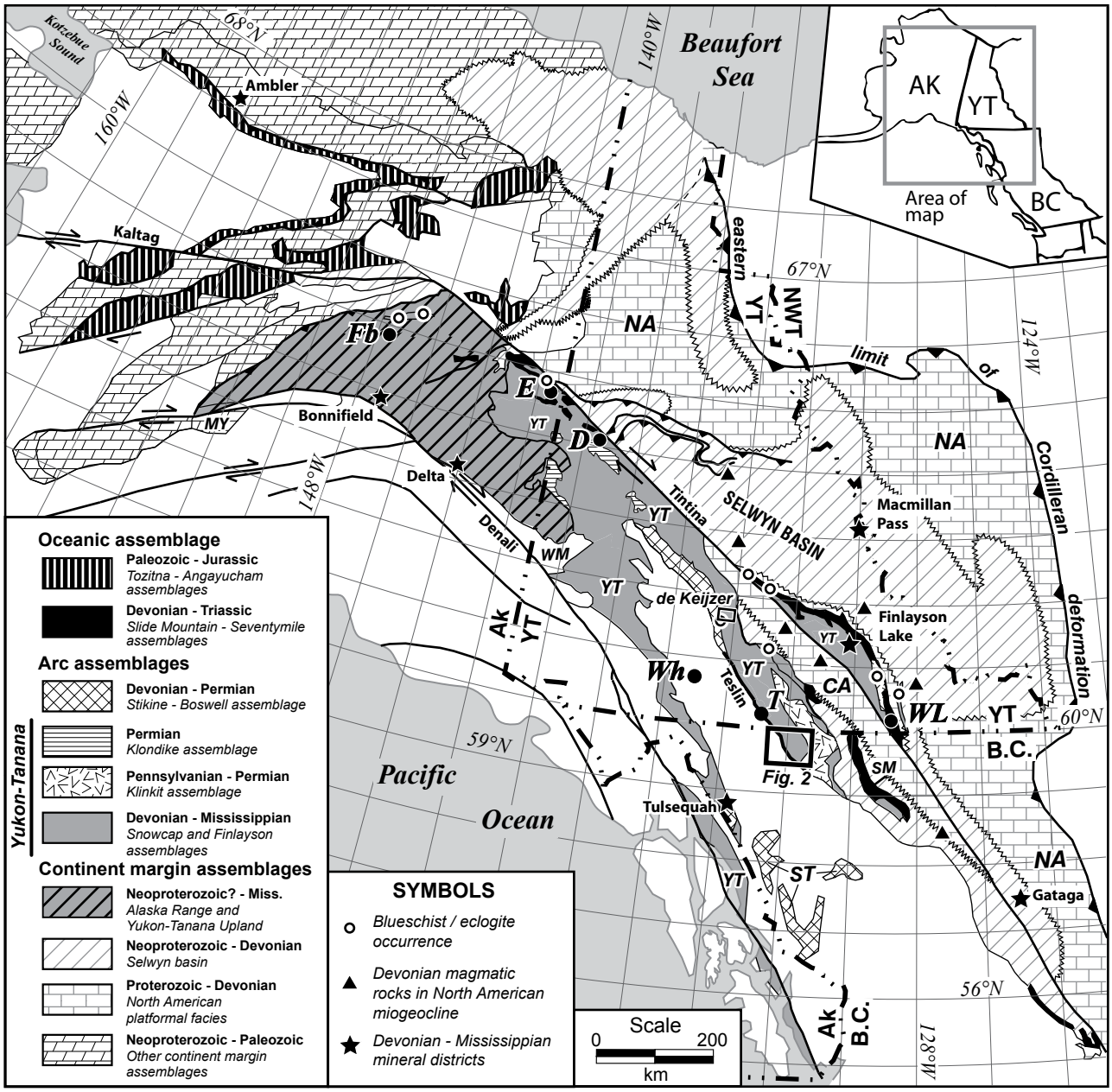

Figure 1. *Location map showing the regional geological setting of the Big Salmon Complex in the northern Cordillera (modified after Wheeler and McFeely, 1991; Silberling* et al.*, 1992; Foster* et al.*, 1994). It is bounded to the southwest by the Teslin fault (indicated) and to the southeast by the Simpson Peak batholith and other plutons in the Jennings River area. Terrane designations are: YT = Yukon-Tanana; CA = Cassiar; SM = Slide Mountain; ST = Stikine; WM = Windy McKinley; and NA = North America. Location designations are: D = Dawson; E = Eagle; FB = Fairbanks; T = Teslin; Wh = Whitehorse; YT = Yukon Territory; Ak = Alaska; NWT = Northwest Territory. Carbonate to shale facies transition is denoted by the zig-zag boundary. The study area shown in Figure 2 is indicated. Location of the study of de Keijzer* et al. *(1999) is also shown.*

PAGE PROOFS

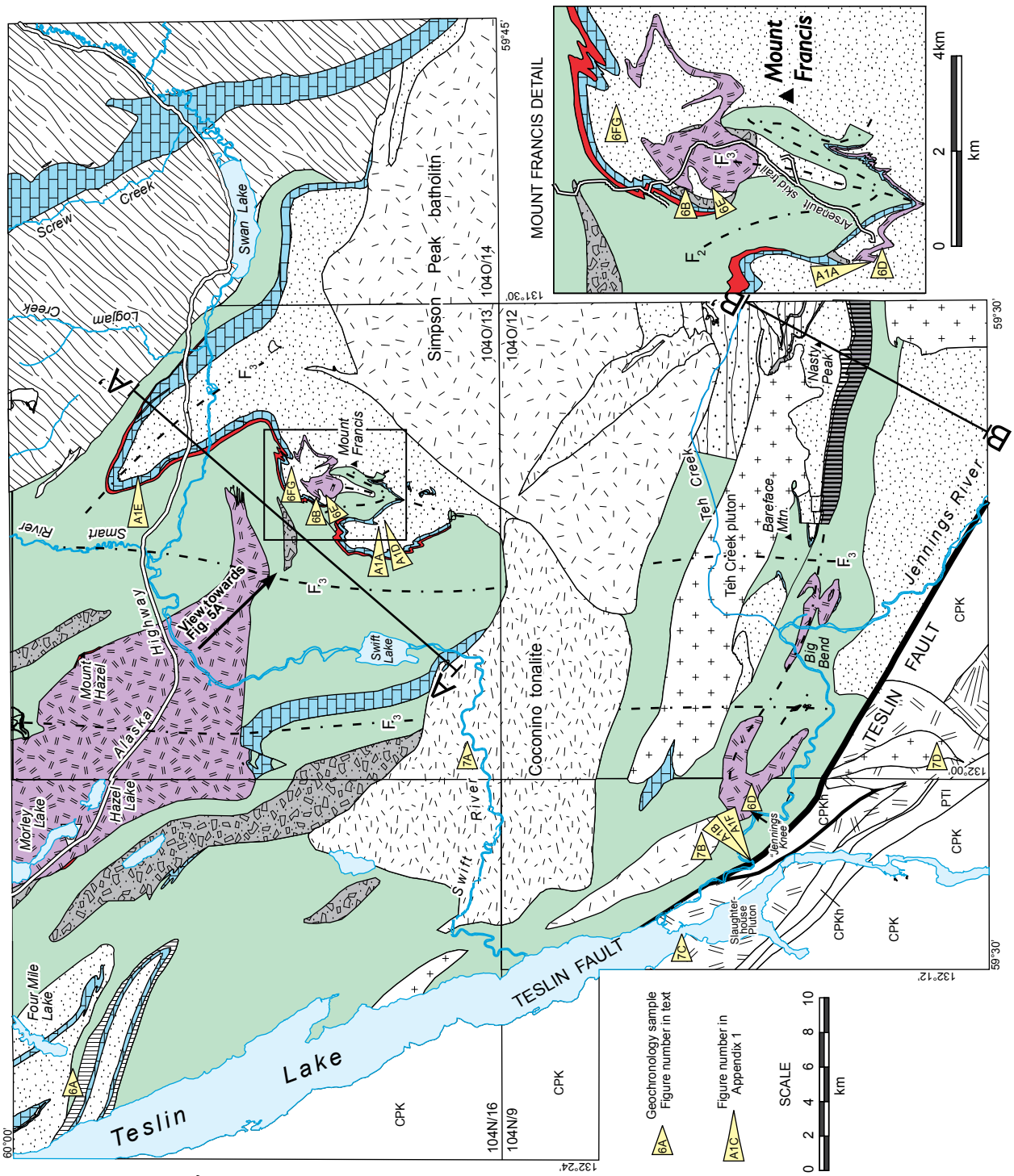

Figure 2. *Generalized geology of the map area (modified after Mihalynuk* et al., *2000), and interpretation of correlations with strata north of the Yukon border (after Colpron* et al., *this volume).*

PAGE PROOFS

mineral wealth that is characteristic of other parts of the Finlayson assemblage. Most of the Big Salmon complex is under-explored for mineral deposits, but locally contains sulphide accumulations interpreted to be syngenetic. Good potential exists for discovery of additional volcanogenic massive sulphide deposits. To fully understand the geological history and to accurately evaluate the mineral potential of the belt, a firm understanding is required of the formative tectonic setting that relate these rocks, subsequent deformational events, and metamorphism and structural fragmentation that disguised and separated them. In this paper we explore deformational events as defined within a surprisingly continuous marker succession in northern British Columbia and southernmost Yukon (Fig. 1), herein called the Jennings marker. We present data that bear on the age of these events and correlate them with events affecting disparate parts of the belt. Finally, we outline a speculative tectonic framework for deposition of the Big Salmon Complex, causes of deformation, and potential affects on dispersal or accumulation of mineral endowment.

The Big Salmon Complex was originally defined by Mulligan (1963) in the Teslin map-area (NTS 105C), and subsequently included by Mihalynuk *et al.* (1998) within the composite Yukon-Tanana terrane (*sensu* Mortensen, 1992; equivalent to the Nisutlin subterrane of Kootenay terrane, *sensu* Wheeler *et al*., 1991a; Gordey and Stevens, 1994). For more than three decades, Big Salmon rocks in British Columbia were included with the oceanic Slide Mountain terrane (Gabrielse, 1969; Wheeler *et al*., 1991b). Three principal characteristics of the Big Salmon Complex have led to its reassignment to the Yukon-Tanana terrane: 1) Big Salmon Complex displays a Yukon-Tanana-like pericratonic character due to a predominance of quartz-rich clastic rocks (see Roots *et al*., this volume) and an evolved εNd signature (+0.5 [basalt] to -26.2 [sandstone]; Creaser *et al*., 1995); 2) the voluminous Smart River metabasalt displays a continental arc geochemical signature (Piercey *et al*., this volume; M. Mihalynuk and J. Peter, unpublished data); 3) rocks of similar character extend along strike from the Big Salmon Complex in British Columbia to those that define the Yukon-Tanana terrane in Yukon (Mortensen, 1992).

In Yukon, rocks related to the Big Salmon Complex were interpreted by Tempelman-Kluit (1979) as a subduction/collisional complex, the Teslin suture zone, comprised of dismembered ophiolite (Anvil allochthon) and siliceous cataclasite (Nisutlin allochthon). Discovery of high pressure eclogite (Erdmer and Helmstaedt, 1983; Erdmer, 1985) supported the collisional concept, and work along strike in the northern Teslin area (Hansen, 1989, 1992a, b; Hansen *et al*. 1989, 1991) appeared to outline a fossil Permo-Triassic subduction zone with offscraped sediments affected by tectonic backflow. More recent work (Stevens, 1992; Stevens and Erdmer, 1993; Stevens and Harms, 1995 and Stevens *et al*., 1996) shows that the Teslin "suture zone" is comprised not of disparate offscraped oceanic sediments, but of continental margin strata (Creaser *et al*., 1995) with relatively coherent stratigraphic relationships, which correlate with the lower to middle units (*sensu* Mortensen, 1992) of the Yukon-Tanana terrane farther north. These workers accordingly renamed the Teslin suture zone as the Teslin tectonic zone. De Keijzer and Williams (1997) mapped apparently coherent strata within the Teslin tectonic zone as a polydeformed nappe.

Within the Big Salmon Complex of northern B.C., a polydeformed nappe can also be mapped, where it is outlined by the distinctive and regionally persistent Jennings marker succession, which extends from Jennings River in British Columbia to northern Morley Lake in Yukon. The Jennings marker is particularly important for regional correlation, and for outlining complex large-scale interference structures that may have more regional implications. It also serves as a benchmark for measuring the amount of along-strike facies variations and structural offsets. It contains evidence of a significant erosional episode, and may provide a key to correlating regional deformational events. It is also of economic significance. A persistent chert-exhalite unit within the Jennings marker, known as the "Old Highway metachert", is a possible exploration target for submarine hydrothermal mineralization. Where regional peak metamorphic conditions have been imprinted on the polydeformed metachert, layers of bright red piedmontite-garnet contrast with white quartz and black pyrolusite to produce a very attractive rock that is quarried for building material.

JENNINGS MARKER SUCCESSION

Four distinctive units comprise the Jennings marker succession (Figs. 2, 3). From oldest to youngest the units are:

1) Smart River metabasalt: 1200+ m of tuffite-dominated, dark green, metamorphosed basalt; mainly lapilli and ash tuff, epiclastic strata and flows; locally displaying good protolith textures (Figs. 4A, DR1A [see footnote 1]). Nowhere is the base of the unit clearly exposed.
2) Old Highway metachert: 0-50 m of thinly bedded, finely laminated manganiferous metachert with muscovite partings. This unit was formerly called "crinkle chert" (Mihalynuk *et al*., 1998), because thin beds or laminae have been deformed to produce millimetre-thick resistant ribs with equally thin micaceous interlayers that are extensively folded by chevron crenulations (crinkles, Figs. 4B, DR2 [see footnote 1]). A pale pink to bright fuchsia colour is produced with increasing piedmontite content (Figs. 4B, C, DR2). Near upper contact of the unit, a Cu-Zn-Fe-Mn-Ba-rich lens several metres long points to the potential for volcanogenic exhalative deposits, confirmed by geochemical analyses that show a significant exhalative component (Mihalynuk and Peter, 2001) and the recent discovery of associated massive sulphide mineralization east of Morley Lake (Mor property; Poliquin, 2004). In rare instances, felsic tuff is apparently mixed with, or occurs intead of the Old Highway metachert (Figs. 2, 3). The lower contact of the metachert is locally gradational with tuffaceous rocks of the Smart River metabasalt.
3) Logjam limestone: 70-300 m of buff to grey weathering limestone with metre-thick tuffaceous and thin centimetre- to decimetre-thick quartzite layers. It is typically massive in the lower sections with rare, silicified horn and colonial corals, bryozoa and crinoids (Fig. 4D). The upper part of the unit contains bright green tuffaceous sedimentary interbeds that grade into carbon-

PAGE PROOFS

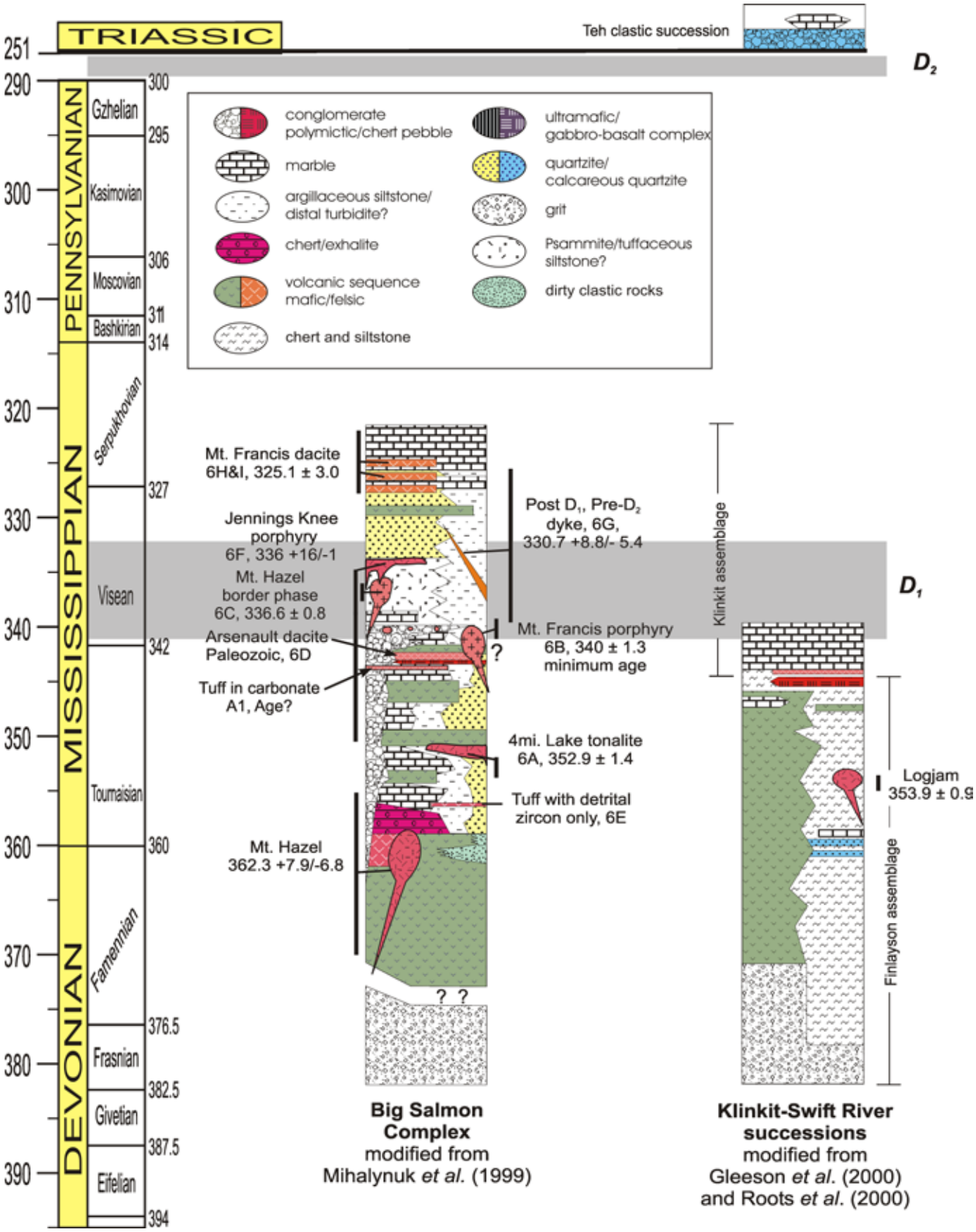

Figure 3. *Stylized time-stratigraphic column showing temporal relations between units (see also Roots* et al.*, this volume; time scale of Okulitch, 2002).*

PAGE PROOFS

ate (Fig. DR1B). At several localities, its base is an abrupt to gradational contact with metachert. Elsewhere, the limestone passes laterally into dark grey tuffaceous argillite, which is in contact with the metachert unit.

4) 0-20 m lenses of polymictic conglomerate (Fig. DR1C) contained within the lower half of the Logjam limestone. The erosional surface atop which the conglomerate was deposited may locally have cut down into the metabasalt, as evidenced by rounded greenstone clasts. However, clasts are commonly

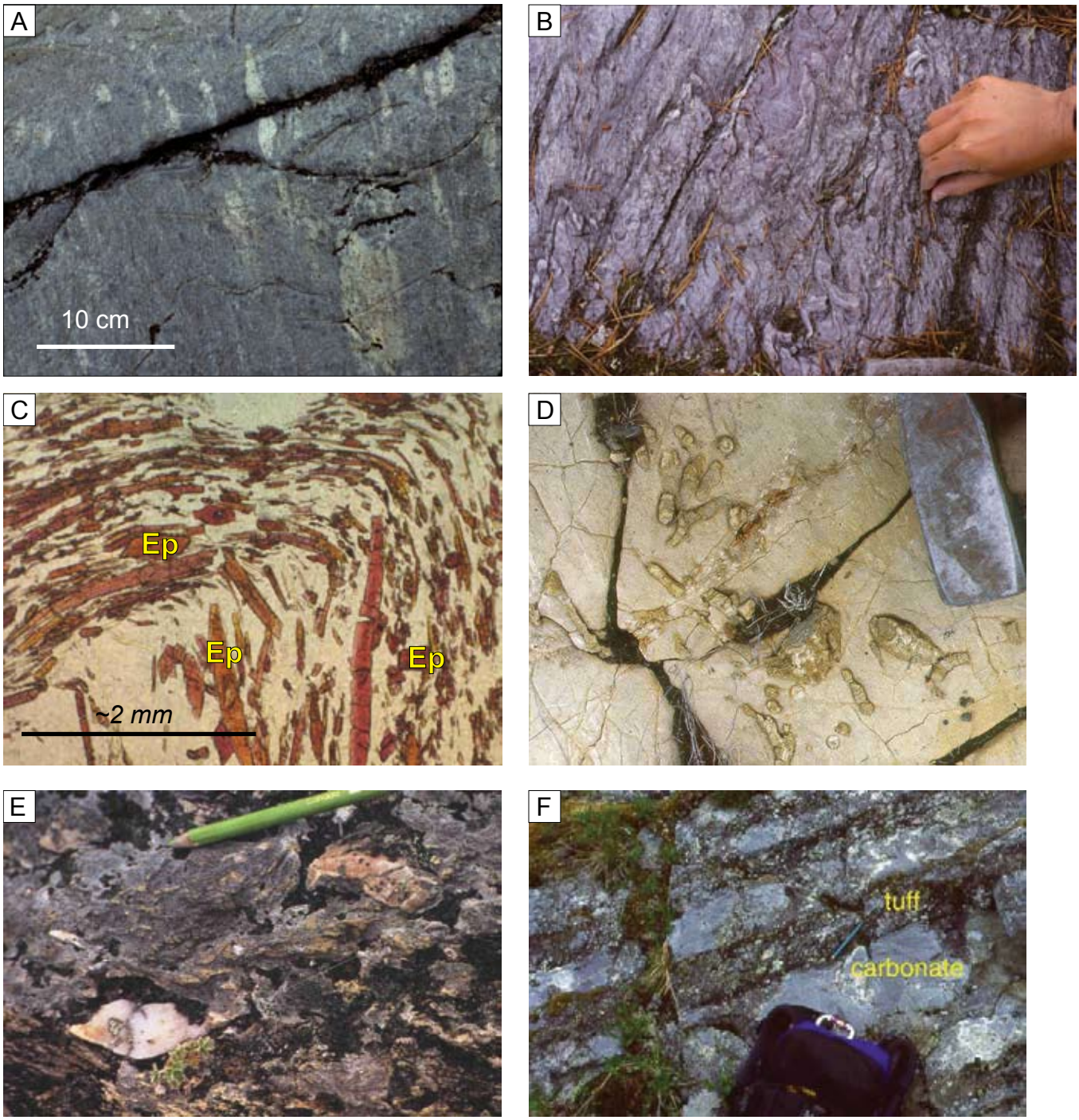

Figure 4. *A) primary volcanic tuffaceous textures in Smart River metabasalt shown by light-coloured, stretched lapilli; B) typical centimetre-scale crenulations in Old Highway metachert; C) plane polarized light photomicrograph of refolded (F_3) quartz–muscovite-piedmontite (yellow to fuschia, Ep) schist; D) silicified ?bryozoa in Logjam limestone; E) polymictic conglomerate within the Logjam limestone, here with angular, recrystallized chert clasts in calcareous matrix; F) 325 Ma tuff interlayered with carbonate in upper mixed package of the Big Salmon Complex.*

PAGE PROOFS

dominated by blue quartz-eye porphyritic intrusive variants that are similar in composition and texture to the marginal phases of a deformed granitoid body known as the Mount Hazel orthogneiss (336.6 ± 0.8 Ma; see Fig. 2), and to the Mount Francis quartz-feldspar porphyry intrusion (*ca*. 340 Ma). Near Mount Francis, beds of recrystallized pebble conglomerate are comprised mainly of fine-grained quartzite clasts, probably recrystallized chert (Fig. 4E).

Overlying the marker succession is a heterolithic, quartz-rich clastic package that contains intervals of metres to tens of metres thick carbonate, mafic and lesser felsic tuff (Fig. 4F), very pure quartzite, carbonaceous quartz granule conglomerate, carbonaceous phyllite, wacke and variations thereof. Data that constrain the ages of these units are presented below.

STRUCTURAL AND METAMORPHIC FRAMEWORK

Five deformational events affected the Big Salmon Complex; four can be identified in outcrop, and an early cryptic event is only evident upon microscopic examination. Evidence of the deformational events is particularly well developed within a peak, transitional greenschist-amphibolite facies metamorphic culmination in which the stable garnet-actinolite metamorphic mineral assemblage is imprinted on a northwest-trending belt of rocks extending from the Mount Francis area to north of Hazel Peak (Fig. 2). In the core of the culmination, protolith textures are destroyed, but on the lower grade flanks, protolith textures are moderately to well preserved (Figs. 4A, DR1A). As recorded by the Jennings marker and bounding rocks, these four megascopic events, as well as an additional microscopic event, are outlined below in chronological order.

Local Deformation Affecting S_0: Cryptic D_i, S_i

An early cryptic deformation event, here designated D_i, is only sporadically recorded in the high grade core zone rocks east of Mount Francis. This cryptic event is expressed mainly as deformed, pre-regional S_1, inclusion trails within quartz, feldspar, garnet and staurolite porphyroblasts (Fig. 5A). Rare relicts of staurolite, andalusite and possibly kyanite represent amphibolite facies, early peak-metamorphic assemblages that have been extensively retrograded to greenschist facies assemblages of epidote, chlorite, muscovite and calcite (Figs. DR1C, D).

The extent and overall effects of this earliest event are largely unknown, because such textures have only been observed in rocks from the flanks of Mount Francis. Mylonitic metasedimentary units separate rocks displaying this early high-grade event from those displaying intact protolith textures a few kilometres to the west. D_i is not recognized in the Jennings marker succession. We tentatively interpret rocks with D_i porphyroblasts as part of a nappe, possibly emplaced during D_1 and bounded by a fault represented by the mylonitic zone.

First Regional Deformational Episode: D_1, F_1, S_1

The earliest regional deformation produced the strong, nearly layer-parallel schistose or phyllitic fabric that dominates the Big Salmon Complex. The earliest regionally recognizable folds and related schistosity in the Big Salmon Complex are designated F_1 and S_1 respectively. In most places, D_1 is manifested as schistosity or phyllitic fabric that is within 10°, and commonly within 3°, of the bedding orientations (Fig. 5B, compare Figs. 5C and E), and is transposed by S_2. Widespread nearly bedding-parallel S_1 foliation is probably due to high-amplitude isoclinal folding. Strong transposition of S_0 is shown by microscopic intrafolial isoclines (Fig. 5B). Within most of the Big Salmon Complex, D_1 produced S_1, the dominant schistose fabric. First phase fabrics are modified but not totally overprinted by second and third phase folds and fabrics.

Second Regional Deformational Episode: D_2, F_2, S_2

F_2 folds are ubiquitous and are synchronous with the peak of regionally-developed M_2 metamorphism. They are outlined by deformation of the S_1 fabric into parabolic or chevron folds with slightly curved limbs that are open to tight, gently inclined to upright, subhorizontal to, less commonly, steeply plunging (Figs. 5E, F, G). F_2 folds are most commonly observed with wavelengths and amplitudes in the range of 1-10 m. Larger F_2 folds are suggested by regional outcrop patterns, for example on the western flank of Mount Francis (Fig. 6A). Locally, refolding by F_3 has decreased F_2 interlimb angles to nearly recumbent and tight to isoclinal (Fig. 6B). Rarely, F_3 has caused axial-normal flattening parallel with F_2 fold hinges, and increased F_2 interlimb angles (Fig. 5D).

D_2 fabrics are best developed in high grade core zone rocks; in lower grade rocks, S_2 schistosity is not everywhere developed. However, axial-parallel schistosity, designated here as S_2, can be observed almost everywhere there are outcrop-scale F_2 folds. Well-developed, shallowly southeast-plunging mineral elongation lineations (average N168/20, not shown in Fig. 5) are parallel to F_2 hinge lines. However, they cannot everywhere be distinguished from folds and mineral lineations developed during D_1. Contoured poles to S_2 show a weakly multi-modal distribution (Pi girdle pole: N150/24, Fig. 5I), reflecting the variable southwest and northeast vergence

Figure 5. *(facing page) Structural history and features of the Big Salmon Complex. Stereonet plots show contoured data density in units of percent of data points per one percent area. A) photomicrograph of contorted internal schistosity (S_1) in garnet (plane polarized light); B) intrafolial isocline within S_1 (plane polarized light); C) poles to bedding (S_0); D) second phase fold styles in piedmontite schist (F_2); E) poles to the first foliation (S_1); F) mineral lineations (L_{M1}); G) minor fold hinge line orientations – mainly F_2 parasitic folds; H) style of F_3 folds; I) second schistosity (S_2); J) clast elongation lineations (L_e); K) fourth phase and ?younger fold styles (F_4); L) C-plane orientations in Charlie Cole pluton (contoured), and kink band orientations with estimated σ1 and σ3 orientations; M) third foliation (S_3).*

PAGE PROOFS

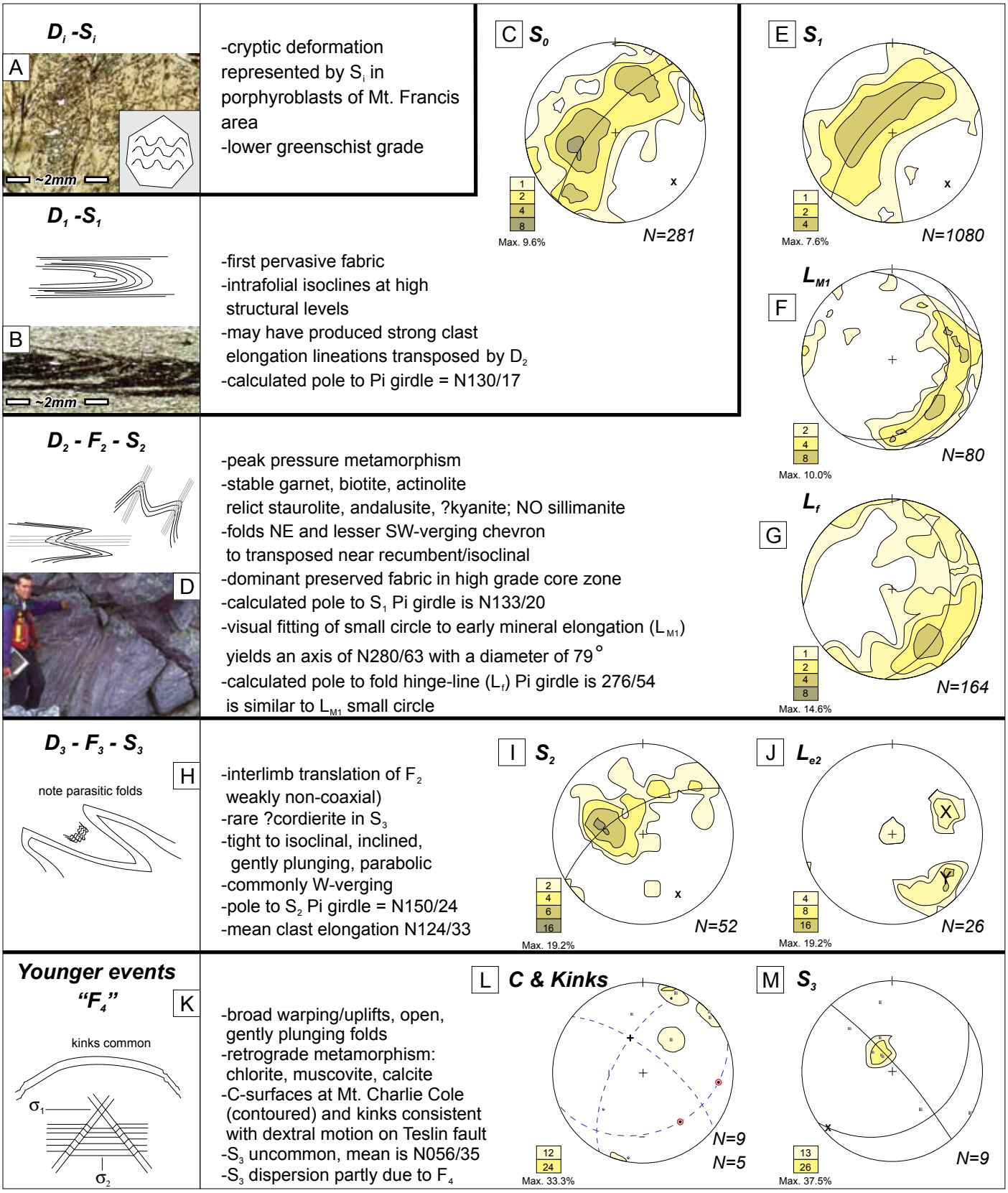

Figure 5. *Caption on facing page.*

PAGE PROOFS

displayed by these relatively cylindrical folds, as well as reorientation by F_3 folds (*e.g.*, Fig. 5J).

Elongation lineation orientations (L_{e2}, Fig. 5J), mainly stretched pebbles and lapilli, represent the finite D_2 strain ellipse, and are denoted L_{e2}. However, deformed clast shapes undoubtedly represent integration of incremental D_1 strain. L_{e2} lineations generally fall into one of two populations (X and Y on Fig. 5J); population "X" is at high angles to S_1-S_2 intersections and the pole to the S_2 Pi girdle. L_{e2X} are probably the product of flexural slip folding, having formed subparallel to the D_2 tectonic transport direction. L_{e2} population "Y" was probably elongated parallel to fold axes, probably near the cores of large-scale F_2 folds. D_2 fabrics are deformed by third-phase, mountain-scale folds attributed to D_3 (Fig. 6A).

Third Regional Deformational Episode: D_3, F_3, S_3

F_3 folds are important regionally north of the Simpson Peak batholith. Northeast of Mount Francis, a large-scale recumbent F_3 synform involves the Jennings marker and refolds earlier F_2 folds (Figs. 6A, C). F_3 folds are close to isoclinal, subhorizontal, and inclined to overturned (Fig. 5I). They are semi-elliptical to parabolic in shape with high amplitudes and relatively straight limbs (Fig. 5H). North of "Nasty Peak", F_3 folds are overturned to the northeast (Fig. 6D) and have apparently been developed in two stages (F_{3a} and F_{3b}). F_{3b} folds near Butsih Creek are inclined and close; they overprint recumbent, nearly isoclinal F_{3a} folds.

Parasitic folds, and a strong axial planar fabric, are common and can be recognized in mountain-scale F_3 folds. However, it is not always possible to distinguish F_2 and F_3 schistosities, unless fold-fabric relationships can be established at the outcrop. S_3 can be recognized petrographically, because it formed during retrograde M_3 metamorphism and is commonly outlined by the growth of chlorite, muscovite, calcite ± epidote. In some cases, chlorite-lined S_3 surfaces can be distinguished in outcrop. The dispersion of poles to S_2 shown in Fig. 5I is the result of F_3 folding, and a concentration of measurements from domains most strongly affected by D_4 kinking and warping, especially in the high-grade core region.

Fourth Deformation: Local F_4

F_4 folds are broad warps with little preferred orientation, although a Pi girdle defined by sparse S_3 orientation data (N=9) is suggestive of folds with an axis orientation of N229/05 (Fig. 5M). Local strong development of kink bands in chlorite and muscovite schist (retro-

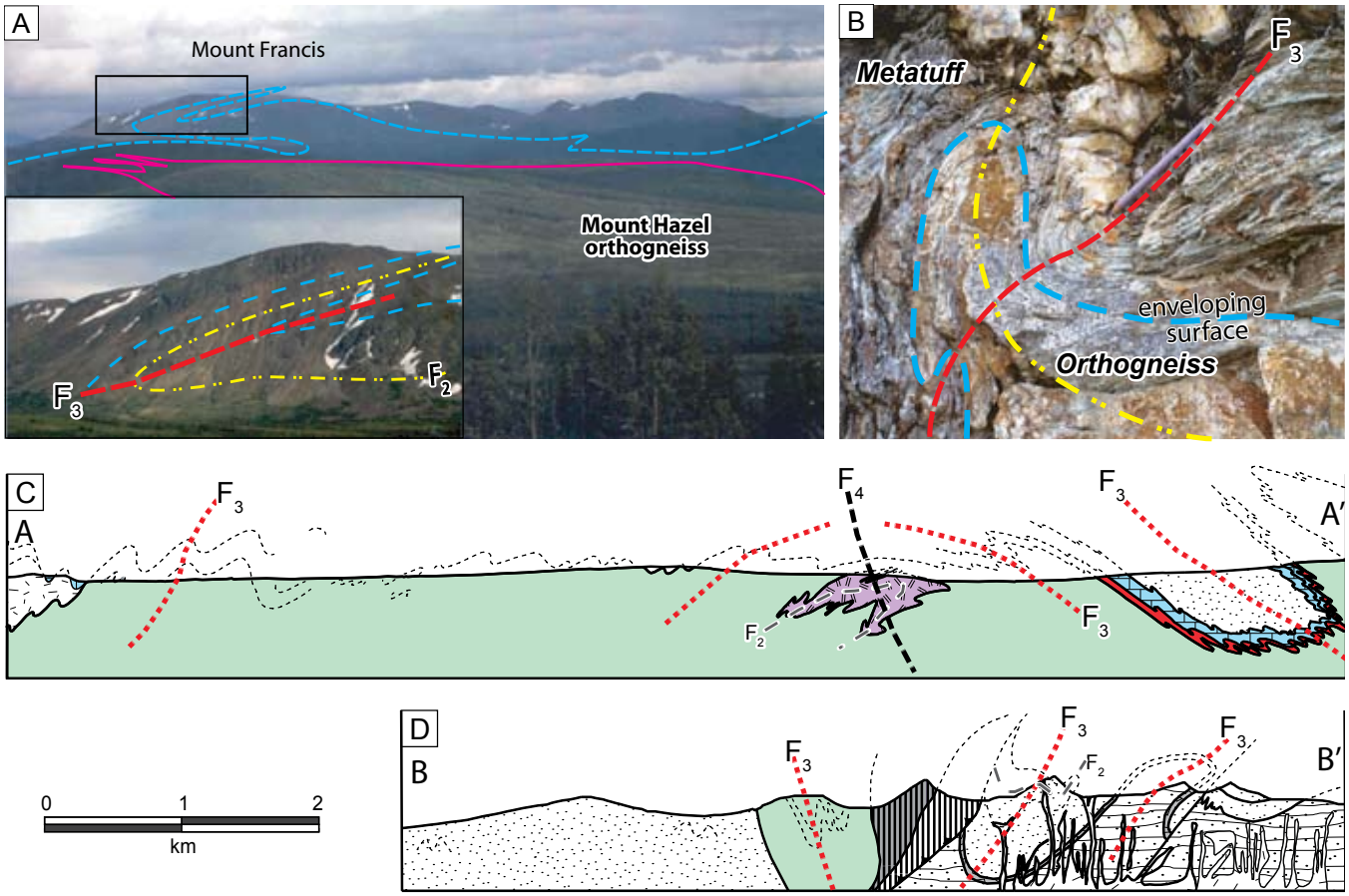

Figure 6. *Structural style shown in representative cross sections: A) Mount Francis refolded fold photograph with trace of greenstone superimposed; inset shows detail of an F_2 fold refolded by F_3; B) refolded Four Mile Lake tonalite dike; C) cross-section of the Mount Francis and Logjam Creek areas (after Mihalynuk* et al.*, 2000); D) "Nasty Peak" area cross-section (simplified after Mihalynuk* et al.*, 2001). See Figure 2 for location of cross-sections shown in C and D; both are 2.5 times the scale of Figure 2.*

PAGE PROOFS

grade M_4 metamorphism) formed during this late warping (Figs. 5K, L).

Ductile shear fabrics overprint more than 2 km^2 of the 57.3 +0.4/-0.6 Ma Charlie Cole pluton (see below), but are not recognized in rocks of the Big Salmon Complex. These moderate to steeply southwest-dipping fabrics (Fig. 5L), together with F_4 warps and kinks, may be related to motion on the nearby Teslin fault. An eastern strand of the Teslin fault is shown by Gordey (1992; Gordey and Stevens, 1994) as plugged by a 109 Ma pluton near the town of Teslin (Fig. 1). If strain across the fault is responsible for the fabrics in the Charlie Cole pluton, motion must have occurred west of the 109 Ma pluton subsequent to 57 Ma.

GEOCHRONOLOGY

U-Pb dating has revealed the relative ages of units within the Big Salmon Complex, as well as broad age limits for deformational events. In this section, we outline new or revised isotopic age data (Table 1, Figs. 7, 8). All errors are reported at the 2σ level. Incomplete or ambiguous age determinations are only presented in the Appendix 1 (see footnote 1). Geochronologic data from surrounding units are reviewed in Roots *et al.* (this volume). U-Pb sample locations are shown on Figure 2.

Analytical Techniques

All samples except one were processed at the Geochronology Laboratory, University of British Columbia (UBC). Sample 99JN-20-1 was processed at the Radiogenic Isotope Facility, University of Alberta (U of A), and details of the U-Pb procedures are outlined in Heaman *et al.* (2002). Zircon was separated from an approximately 25 kg sample employing conventional crushing, grinding and Wilfley table techniques, followed by final concentration using heavy liquids and magnetic separations. Mineral fractions for analysis were selected based on grain morphology, quality, size and magnetic susceptibility. All zircon fractions analysed at UBC were abraded prior to dissolution (except where noted below) to minimize the effects of post-crystallization Pb-loss, using the technique of Krogh (1982). HF leaching techniques performed on five fractions from one sample (Arsenault dacite, UBC) are listed in Friedman *et al.* (2001). All samples were dissolved in concentrated HF and HNO_3 in the presence of a mixed $^{233\text{-}235}U$-^{205}Pb tracer (^{235}U-^{205}Pb tracer at U of A). Separation and purification of Pb and U employed ion exchange column techniques modified slightly from those described by Parrish *et al.* (1987). Pb and U were eluted separately and loaded together on a single Re filament using a phosphoric acid-silica gel emitter. Isotopic ratios were measured using a modified single collector VG-54R thermal ionization mass spectrometer equipped with a Daly photomultiplier (UBC) and VG354 (U of A). Most measurements were done in peak-switching mode on the Daly detector. U and Pb analytical blanks were in the range of 1 pg and 2-7 pg (UBC) and 0.5-1.0 pg and 1-3 pg (U of A), respectively, during the course of this study. U fractionation was determined directly on individual runs using the $^{233\text{-}235}U$ tracer, and Pb isotopic ratios were corrected for mass discrimination using empirically derived values of 0.12%/amu and 0.35%/amu for Faraday and Daly runs, respectively, based on replicate analyses of the NBS-981 Pb standard and the values recommended by Thirlwall (2000). For isotopic analyses measured at U of A, corrections for Pb (0.09%/amu) and U (0.16%/amu) mass discrimination are based on repeat measurement of the NBS-981 and U500 standards. All analytical errors were numerically propagated through the entire age calculation using the technique of Roddick (1987). Analytical data are reported in Table 1 and Table A1 of Appendix 1 (see footnote 1). Concordia intercept ages and associated errors (except in case where specifically noted) were calculated using a modified version the York-II regression model (wherein the York-II errors are multiplied by the MSWD) and the algorithm of Ludwig (1980).

Metamorphosed Rocks

U-Pb isotopic age determinations were conducted on a suite rocks from the Big Salmon Complex and younger intrusions within the study area (locations shown on Fig. 2). Results from two of these samples are reported in Roots *et al.* (2002). Six of the samples did not yield protolith ages, or yielded ambiguous results (Appendix 1). Eleven samples yielded protolith ages and are the focus of this section, listed from oldest to youngest.

Four Mile Lake Tonalite, 352.9 ± 1.4 Ma (Fig. 7A)

Medium-grained tonalite is infolded with metabasalt about 1.5 km southwest of Four Mile Lake (Fig. 2). Both units display probable D_1 foliation that is affected by D_2 and D_3 folds (Fig. 6B). At the contact, the tonalite is porphyritic, apparently preserving an original, but transposed chilled contact.

Zircons are clear to turbid, pale pink, stubby prisms with irregular edges due to resorption. Five fractions comprising six to 15 abraded grains each were analysed. An age estimate of 352.9 ± 1.4 Ma is based upon the total range of $^{206}Pb/^{238}U$ ages for fractions A and C, which give the oldest overlapping results. Slightly younger results for other fractions are thought to reflect minor Pb loss from the analysed grains.

Mount Francis Quartz-Feldspar Porphyry, Minimum Age of 340 ± 1.3 Ma (Fig. 7B)

A porphyry stock containing feldspar and blue quartz eyes appears to intrude the Jennings marker succession near Mount Francis. It records two phases of deformation: an early foliation and superimposed strong crenulation fabric. Both are outlined by replacement epidote. Chloritized biotite is evident along with abundant tourmaline.

Contact relations strongly suggest that the porphyry cuts the stratigraphic interval occupied by the upper greenstone unit and possibly the Old Highway metachert, Logjam limestone, and a clastic unit that may interfinger with the limestone. Contacts are not exposed, but intrusive relationships are supported by indications of thermal metamorphism in the adjacent units. Furthermore, the metachert and lower limestone appear to have been largely removed by erosion, and are represented by a conglomerate containing automobile-sized blocks of recrystallized Logjam limestone and sparse cobbles of quartzite, mixed with intrusive boulders that locally dominate the

PAGE PROOFS

Table 1. U-Pb ID-TIMS analytical data for rocks from the Big Salmon Complex.

Fraction[1]	Wt	U[2]	Pb*[3]	^{206}Pb[4]	Pb[5]	Th/U[6]	Isotopic ratios (±1σ,%) [7]			Apparent ages (±2σ,Ma) [7]		
	(µg)	(ppm)	(ppm)	^{204}Pb	(pg)		$^{206}Pb/^{238}U$	$^{207}Pb/^{235}U$	$^{207}Pb/^{206}Pb$	$^{206}Pb/^{238}U$	$^{207}Pb/^{235}U$	$^{207}Pb/^{206}Pb$
Four Mile Lake tonalite, MMI97-30-6: 352.9 ± 1.4 Ma; 650000 E, 6650000N, UTM Zone 8												
A, 6, s, r	14	106	6	1716	3	0.43	0.05620 (0.15)	0.4147 (0.42)	0.05351 (0.37)	352.5 (1.0)	352.2 (2.5)	351 (17)
B, 9, s, r	13	84	5	1287	3	0.55	0.05583 (0.20)	0.4117 (0.68)	0.05348 (0.62)	350.2 (1.4)	350.1 (4.0)	349 (28)
C, 12, s, r, tu	14	106	6	2289	2	0.63	0.05630 (0.16)	0.4170 (0.41)	0.05372 (0.36)	353.1 (1.1)	353.9 (2.4)	359 (16)
D, 15, s, r, tu	13	158	9	1962	4	0.57	0.05598 (0.12)	0.4127 (0.49)	0.05347 (0.44)	351.1 (0.8)	350.8 (2.9)	349 (20)
E, 14, s, r, tu	12	144	8	1515	4	0.57	0.05564 (0.15)	0.4113 (0.51)	0.05361 (0.46)	349.1 (1.1)	349.8 (3.0)	355 (21)
Mt. Francis quartz-feldspar porphyry, MMI00-6-12: minimum age of 340.0 ± 1.3 Ma; 348065E, 6636800N, UTM Zone 9												
A1, 2, s, r	8	55	3	431	4	0.29	0.05416 (0.19)	0.3994 (0.86)	0.05348 (0.78)	340.0 (1.3)	341.2 (5.0)	349 (35)
A2, 5, s, r	6	273	15	1708	3	0.35	0.05296 (0.16)	0.3988 (0.32)	0.05462 (0.26)	332.6 (1.0)	340.8 (1.8)	397 (11)
B1, 1, s, r	9	111	6	957	4	0.31	0.05356 (0.23)	0.4038 (0.44)	0.05467 (0.37)	336.4 (1.5)	344.4 (2.5)	399 (17)
B3, 6, s, r	20	152	8	2095	5	0.33	0.05140 (0.18)	0.3869 (0.27)	0.05459 (0.16)	323.1 (1.1)	332.1 (1.5)	395.4 (7.3)
Mt. Hazel pluton, 99JN32-3: lower intercept age, 336.6 ± 0.8 Ma; MSWD=0.71; 663200E, 6851300N UTM Zone 8												
A, 7, s	15	380	21	1504	13	0.61	0.05192 (0.15)	0.3842 (0.27)	0.05368 (0.17)	326.3 (0.9)	330.1 (1.5)	357.5 (7.8)
B, 13, s	18	207	13	606	23	0.49	0.05873 (0.16)	0.4989 (0.39)	0.06161 (0.29)	367.9 (1.1)	411.0 (2.6)	661 (12)
C, 15, s	10	215	12	4044	2	0.50	0.05391 (0.11)	0.3990 (0.23)	0.05367 (0.18)	338.5 (0.7)	340.9 (1.3)	357.3 (8.1)
D, 50, s	10	201	11	3105	2	0.55	0.05353 (0.16)	0.3925 (0.30)	0.05318 (0.26)	336.1 (1.0)	336.2 (1.7)	336 (12)
Jennings Knee quartz porphyry, 99JN27-5: 336 +16/-1 Ma; 667850E, 6613500N, UTM Zone 8												
A, 5, y	10	280	17	846	11	0.89	0.05354 (0.13)	0.3925 (0.45)	0.05317 (0.39)	336.2 (0.8)	336.2 (2.6)	336 (18)
B, 20, y	13	158	9	561	12	0.53	0.05309 (0.21)	0.3892 (0.75)	0.05317 (0.69)	333.5 (1.4)	333.9 (4.3)	336 (31)
C, 20, y	13	179	10	842	10	0.61	0.05399 (0.17)	0.4206 (0.44)	0.05650 (0.37)	338.9 (1.1)	354.8 (2.7)	472 (16)
D, 40, y	14	286	16	1304	10	0.71	0.05129 (0.32)	0.3796 (0.43)	0.05368 (0.28)	322.4 (2.0)	236.7 (2.4)	358 (13)
Post D2, pre-D3 dike, MMI97-17-7: upper intercept age, 330.7 +8.8/-5.4 Ma; MSWD=0.16; 348000E, 6636000N, UTM Zone 9												
A, 4	30	189	10	1581	12	0.35	0.05130 (0.16)	0.3750 (0.26)	0.05302 (0.20)	322.5 (1.0)	323.3 (1.5)	329.6 (9.1)
C, 16, e	50	258	13	2525	16	0.40	0.04863 (0.10)	0.3557 (0.20)	0.05305 (0.13)	306.1 (0.6)	309.0 (1.1)	330.8 (5.7)
D, 40, f	80	348	18	5079	18	0.35	0.05189 (0.12)	0.3821 (0.18)	0.05340 (0.10)	326.1 (0.8)	328.6 (1.0)	346.0 (4.3)
E, ~10	12	261	13	3497	3	0.46	0.04720 (0.12)	0.3450 (0.20)	0.05302 (0.12)	297.3 (0.7)	301.0 (1.0)	329.5 (5.3)
F, ~10, y, eq	10	322	16	2313	4	0.47	0.04768 (0.17)	0.3481 (0.27)	0.05296 (0.18)	300.2 (1.0)	303.3 (1.4)	327.2 (8.3)
G, ~15, eq	11	294	16	3379	3	0.41	0.05205 (0.12)	0.3806 (0.22)	0.05304 (0.16)	327.1 (0.8)	327.5 (1.2)	330.6 (7.2)
T1, ~30, y, f	310	51	2	39	1510	0.38	0.03071 (2.5)	0.2191 (8.9)	0.05173 (7.5)	195.0 (9.5)	201 (33)	274 (311/385)
T2, ~30, y, f	360	38	1	59	646	0.38	0.03038 (1.2)	0.2165 (4.5)	0.05169 (3.8)	192.9 (4.7)	199 (16)	272 (164/182)
Mt. Francis tuff, MMI97-35-1a: 325.1 ± 3.0 Ma; 349700E, 6638300N, UTM Zone 9												
A, 21	67	450	29	11032	10	0.52	0.06041 (0.09)	0.5265 (0.15)	0.06321 (0.08)	378.1 (0.7)	429.5 (1.1)	715.2 (3.4)
B, 17	36	361	16	3496	10	0.52	0.04333 (0.10)	0.3163 (0.18)	0.05294 (0.10)	273.5 (0.5)	279.0 (0.9)	326.0 (4.5)
C, 23	38	493	26	9843	6	0.56	0.05042 (0.14)	0.3677 (0.19)	0.05290 (0.09)	317.1 (0.8)	317.9 (1.0)	324.3 (4.1)
D, ~30, f	10	592	33	5489	4	0.63	0.05248 (0.10)	0.3849 (0.17)	0.05320 (0.11)	329.7 (0.6)	330.7 (1.0)	337.4 (4.8)
E, 2	5	292	9	1021	3	0.49	0.03105 (0.14)	0.2166 (0.29)	0.05060 (0.22)	197.1 (0.6)	199.1 (1.1)	223 (10)
F, 5	7	493	30	2902	4	0.58	0.05577 (0.11)	0.6271 (0.18)	0.08156 (0.11)	349.8 (0.8)	494.3 (1.4)	1234.9 (4.4)
G, 8, eq	7	470	18	2041	4	0.41	0.03776 (0.14)	0.3042 (0.23)	0.05843 (0.17)	239.0 (0.7)	269.7 (1.1)	546.0 (7.3)
H, 13	9	490	25	3579	4	0.53	0.04869 (0.15)	0.4661 (0.22)	0.06943 (0.13)	306.5 (0.9)	388.5 (1.4)	911.5 (5.3)
Mt. Francis tuff, MMI97-35-1b: 325.1 ± 3.0 Ma; 349700E, 6638300N, UTM Zone 9												
A, 3, s	7	210	12	3316	1	0.60	0.05159 (0.17)	0.3766 (0.36)	0.05294 (0.30)	324.3 (1.1)	324.5 (2.0)	326 (14)
B, 5	11	179	10	3912	2	0.57	0.05203 (0.25)	0.3799 (0.52)	0.05296 (0.47)	327.0 (1.6)	327.0 (2.9)	327 (21)
C, 10, tu	9	265	14	2590	3	0.51	0.04921 (0.17)	0.3627 (0.24)	0.05345 (0.15)	309.7 (1.1)	314.2 (1.3)	348.0 (6.7)
D, 13	12	362	19	5637	2	0.54	0.05012 (0.17)	0.3727 (0.28)	0.05394 (0.22)	315.3 (1.1)	321.7 (1.5)	368 (10)
Coconino tonalite, MMI97-33-1: 197.9 +5.1/-0.5 Ma; 334050E, 6630000N, UTM Zone 9												
A, 8, m, eq	80	149	5	1658	14	0.51	0.03101 (0.10)	0.2140 (0.22)	0.05006 (0.15)	196.8 (0.4)	196.9 (0.8)	198.0 (6.9)
B, 5, e	40	151	5	1904	6	0.59	0.03118 (0.12)	0.2153 (0.23)	0.05007 (0.18)	197.9 (0.5)	198.0 (0.8)	198.0 (8.3)
C, 20, e	16	201	7	1284	5	0.59	0.03064 (0.19)	0.2115 (0.41)	0.05006 (0.35)	194.6 (0.7)	194.8 (1.5)	198 (16)
D, 17, t	16	239	8	1666	5	0.57	0.03089 (0.20)	0.2133 (0.44)	0.05008 (0.40)	196.1 (0.8)	196.3 (1.6)	199 (19)
T1, ~30, y, f	430	44	2	69	733	1.99	0.03072 (0.95)	0.2120 (3.5)	0.05005 (3.0)	195 (3.7)	195 (13)	197 (134/146)
T2, ~30, y, f	440	99	5	136	724	2.76	0.03085 (0.44)	0.2132 (1.6)	0.05011 (1.3)	195.9 (1.7)	196.2 (5.6)	200 (60/62)
Teslin Zone syenite, 99JN-20-1: lower intercept age, 178.4 ± 3.1 Ma; 664900E, 6616800N, UTM Zone 8												
A, 1	9	197	7	351	10	0.51	0.02897 (0.23)	0.2005 (0.98)	0.05020 (0.91)	184.1 (0.8)	185.6 (3.4)	204 (42)
B, 24	10	703	23	863	16	0.30	0.03034 (0.22)	0.2200 (0.37)	0.05261 (0.27)	192.7 (0.8)	201.9 (1.4)	312 (12)
C, 1	2	764	21	814	4	0.16	0.02818 (0.19)	0.1936 (0.65)	0.04982 (0.59)	179.1 (0.6)	179.7 (2.2)	187 (28)

PAGE PROOFS

Table 1. continued

Fraction[1]	Wt	U[2]	Pb*[3]	^{206}Pb[4]	Pb[5]	Th/U[6]	Isotopic ratios (±1σ,%) [7]			Apparent ages (±2σ,Ma) [7]		
	(µg)	(ppm)	(ppm)	^{204}Pb	(pg)		$^{206}Pb/^{238}U$	$^{207}Pb/^{235}U$	$^{207}Pb/^{206}Pb$	$^{206}Pb/^{238}U$	$^{207}Pb/^{235}U$	$^{207}Pb/^{206}Pb$
Slaughterhouse pluton titanite, MMI97-16-3: ~77 Ma minimum age; 657420E, 6618300N, UTM Zone 8												
T1, ~15, y, f	70	285	3	136	129	0.07	0.01199 (0.46)	0.0795 (1.7)	0.04805 (1.4)	76.9 (0.7)	77.6 (2.5)	102 (66/68)
Charlie Cole pluton, MMI99-23-4: lower intercept age, 57.3 +0.4/-0.6 Ma; MSWD=0.60; 335801E, 6598990N, UTM Zone 9												
A, 2, e	10	1332	11	588	13	0.14	0.00883 (0.14)	0.0579 (0.40)	0.04758 (0.31)	56.7 (0.2)	57.2 (0.4)	78 (15)
B, 4, s	88	839	7	1505	29	0.18	0.00922 (0.14)	0.0609 (0.25)	0.04785 (0.16)	59.2 (0.2)	60.0 (0.3)	91.9 (7.6)
C, 5, s	31	380	3	414	17	0.21	0.00907 (0.21)	0.0758 (0.71)	0.06056 (0.60)	58.2 (0.2)	74.2 (1.0)	624 (26)
D, 11, s	52	838	7	1202	21	0.23	0.00896 (0.14)	0.0583 (0.31)	0.04717 (0.23)	57.5 (57.5 (0.2)	57.5 (0.3)	58 (11)
E, 20, e	41	1156	10	1270	22	0.22	0.00900 (0.13)	0.0588 (0.30)	0.04738 (0.22)	57.8 (0.2)	58.0 (0.3)	69 (11)

[1]Fraction identifier: zircon: A, B etc, or A1, A2, B1, B2, etc; titanite: T1, T2, etc. Fraction ID followed by number or approximate number of grains or fragments analysed. All analysed zircon grains were air abraded prior to dissolution except where noted with abbreviation NA. Unless otherwise noted, analysed zircon grains are clear, colourless to pale pink euhedral prisms. Additional abbreviations: a - amber; e - elongate; eq - equant; f - grain fragments; m - multifaceted; o - opaque; pu - purple; r - resorbed; s - stubby; t - tabular; tu - turbid; y - pale yellow; * denotes HF leaching results for sample MMI97-20-3; * - residual grain; 1* - low temperature leachate; 2* - high temperature leachate. Mass of zircon in leachates nominally considered as 1 µg.
[2]U blank correction of 1pg ± 20%; U fractionation corrections were measured for each run with a double ^{233}U-$_{235}U$ spike.
[3]Radiogenic Pb
[4]Measured ratio corrected for spike and Pb fractionation of 0.0035-0.0038/amu ± 20% (Daly collector) which was determined by repeated analysis of NBS Pb 981 standard throughout the course of this study.
[5]Total common Pb in analysis based on blank isotopic composition.
[6]Model Th/U; Th derived from radiogenic ^{208}Pb and $^{207}Pb/^{206}Pb$ age of fraction.
[7]Blank and common Pb corrected; Pb pocedural blanks were <7 pg and U <1 pg. Common Pb isotopic compositions are based on Stacey and Kramers (1975) model Pb at the interpreted age of the rock or the $^{207}Pb/^{206}Pb$ age of the fraction.

conglomerate. These are variably mixed with boulders of the porphyry, which are deposited on an erosional surface that cuts down section into the top of the metabasalt (Figs. 2, 3, DR1E).

Good-quality zircons were extracted from this sample. Several clear, stubby, prismatic grains were selected for analysis and split into four strongly abraded fractions of one to six grains each. The resulting array of data is plotted in Figure 7B (Table 1). Fraction A1 comprising the two largest and clearest grains gives concordant results of 340.0 ± 1.3 Ma ($^{206}Pb/^{238}U$ age), which is considered as a minimum age for the rock. The maximum age is loosely constrained as 384 Ma; the $^{207}Pb/^{206}Pb$ age of fraction A1, 349 Ma plus its associated error of 35 Ma. In the context of concordant fraction A1 discordant results for fractions A2, B1 and B3 indicate that they contain inheritance and underwent subsequent Pb loss.

Mount Hazel Orthogneiss, 336.6 ± 0.8 Ma (Fig. 7C)

Medium-grained, white to light green, deformed muscovite-chlorite-altered granodiorite was sampled approximately 300 m from its contact with the Old Highway metachert. Strong tectonic disruption has produced a gradational contact between the two units, obscuring the original contact relationship, which was probably intrusive. If intrusive, the age of this unit provides a minimum age for the metachert. Zircons from this sample are pale pink, clear to slightly cloudy, euhedral, stubby prisms. Zoning and cores were not observed during grain selection.

Results for four analyzed zircon fractions are plotted on Figure 7C. An age of 336.6 ± 0.8 Ma is based on the lower intercept of a three point regression (including co-linear B, C and D; MSWD = 0.71, upper intercept of 2187 +54/-52 Ma). Fraction D is concordant at the lower intercept age. Relative to concordant D, fraction A, which was not included in the regression, contains inheritance and has undergone Pb loss.

This meta-intrusive body is contiguous with the main part of the Mount Hazel orthogneiss, which has yielded a U-Pb zircon age of 362.3 +7.9/-6.8 Ma on a more interior phase (Mihalynuk *et al.*, 2000b).

Jennings Knee Quartz Porphyry, 336 +16/-1 Ma (Fig. 7D)

Tan to pink, massive to foliated quartz-eye porphyry crops out on an isolated knoll about 2 km northeast of the Jennings River "knee" (Fig. 2). At this locality it is probably intrusive into grey-green tuffaceous rocks, but the contact has been modified by subsequent deformation.

Zircons recovered from a sample of the porphyry are clear, colourless to pale yellow, slightly resorbed stubby prisms. Four strongly abraded fractions were analysed (Fig. 7D), two of which (A and B) are concordant but not overlapping. Younger fraction B is likely to have undergone minor Pb loss, and Pb loss cannot be ruled out for older A. The $^{206}Pb/^{238}U$ age of 336.2 ± 0.8 Ma for A is therefore considered as a minimum age for the rock. The weighted $^{207}Pb/^{206}Pb$ age for fractions A and B of 336.0 ± 15.6 Ma is a reasonable and conservative maximum age. Combining these constraints leads to an assigned age of 336 +16/-1 Ma. Discordant results for fractions C and D indicate systematics involving both inheritance and Pb loss.

Post-D_1, pre-D_2 Dike, 330.7 +8.8/-5.4 Ma (Fig. 7E)

An approximately 0.5 m-thick dike of intermediate composition cuts metasedimentary rocks 2.5 km northwest of Mount Francis. It cuts the early D_1 ductile deformation fabric and is affected by the later D_2 ductile fabric.

Both zircon and titanite were recovered from this sample. Zircons are clear, pale pink euhedral prisms, mostly broken and titanites are pale yellow to clear fragments of euhedral grains. Zircons

PAGE PROOFS

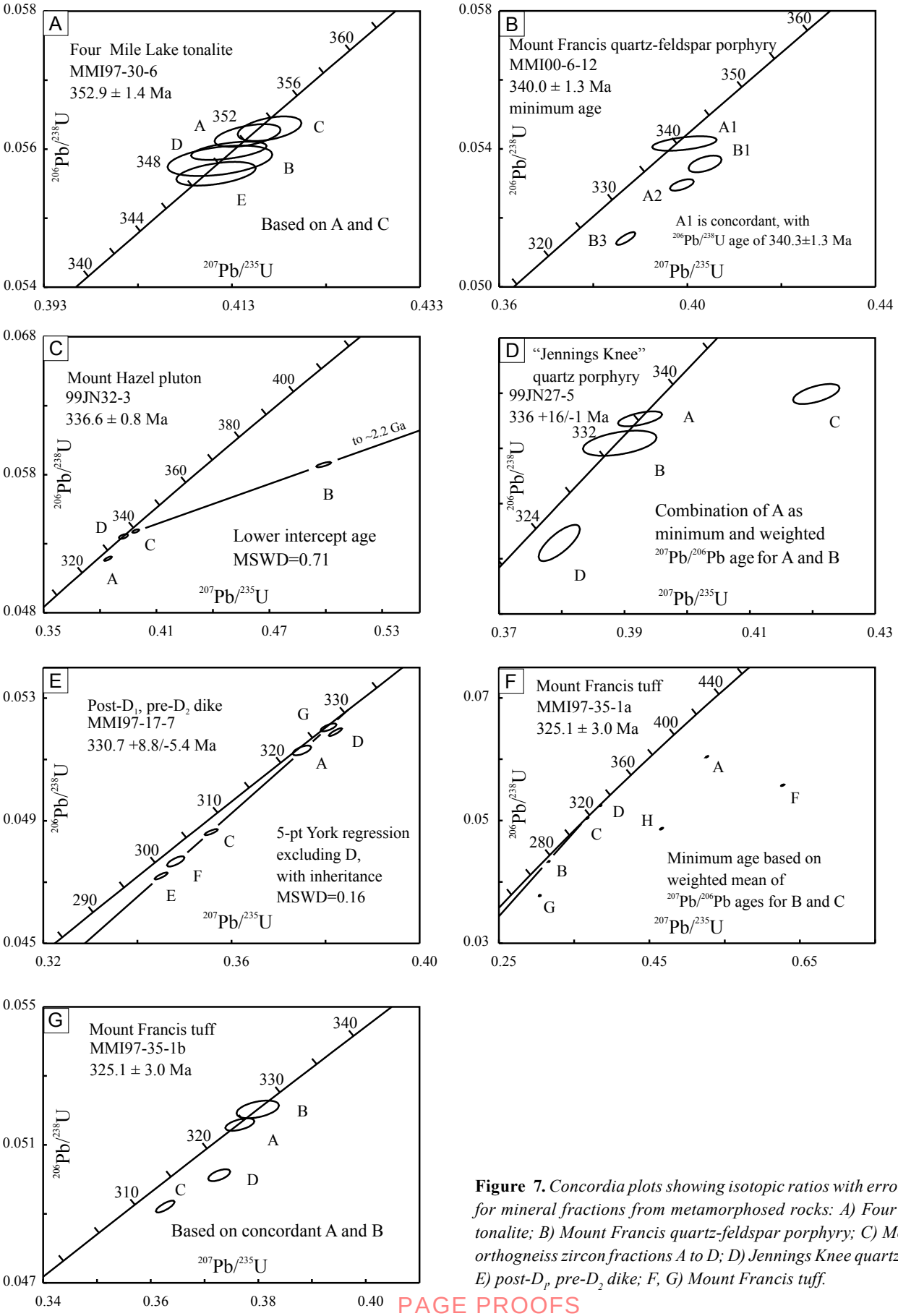

Figure 7. *Concordia plots showing isotopic ratios with error estimates for mineral fractions from metamorphosed rocks: A) Four Mile Lake tonalite; B) Mount Francis quartz-feldspar porphyry; C) Mount Hazel orthogneiss zircon fractions A to D; D) Jennings Knee quartz porphyry; E) post-D_1, pre-D_2 dike; F, G) Mount Francis tuff.*

PAGE PROOFS

are interpreted to have undergone Pb loss. An upper intercept age of 330.7 +8.8/-5.4 Ma is based on a York regression (MSWD = 0.16) through all zircon analyses except D, which is interpreted to contain inheritance (Fig. 7E). Two relatively imprecise titanite analyses intersect concordia at about 190 Ma (not shown on concordia plot). It is unclear whether titanite is magmatic and underwent strong Jurassic Pb loss, or crystallized during a Jurassic event. In either case, elevated Jurassic temperatures are indicated.

Mount Francis Dacite Tuff, 325.1 ± 3.0 Ma (Figs. 7F, G)

Two samples of dacite tuff were collected at a locality on the northern flank of Mount Francis, within the upper heterolithic clastic package approximately 100 m above the Logjam limestone. Data from one of the samples, MMI97-35-1a, is reported here. This sample yielded pale pink, slightly turbid to clear, mostly broken, euhedral prismatic grains. Seven discordant multi-grain analyses show the effects of Pb loss and/or inheritance. Fractions B and C (Fig. 7G; Table 1) are likely to contain no inherited Pb and have only undergone the effects of Pb loss. The weighted mean of $^{207}Pb/^{206}Pb$ ages for these analyses, 325.1 ± 3.0 Ma, provides a reasonable estimate of the minimum age of this sample (MMI97-35-1a); it is in agreement with concordant ID-TIMS U-Pb results for another sample from this unit (MMI97-35-1b) reported by Mihalynuk *et al*. (2000b), but these authors mismatched the concordia plot and data for samples 35-1a and 35-1b. We include the data and corresponding concordia plots for both samples here (Table 1; Figs. 7F, G).

Jurassic and younger granitoids

Coconino Tonalite, 197.9 +5.1/-0.5 Ma (Fig. 8A)

Foliated hornblende-biotite tonalite underlies the low ridges east and south of Coconino Lake. It forms a roughly equidimensional body extending 15 km south of the Swift River. Weakly-oriented, fine-grained biotite forms elongated clots (20%) up to 1cm long after original biotite phenocrysts. Some of the biotite clots are cored with epidote, probably replacing hornblende. Most plagioclase is strongly replaced by epidote and muscovite.

Both zircon and titanite were recovered from this sample. Zircons are high quality, very clear, pale pink, teardrop-shaped,

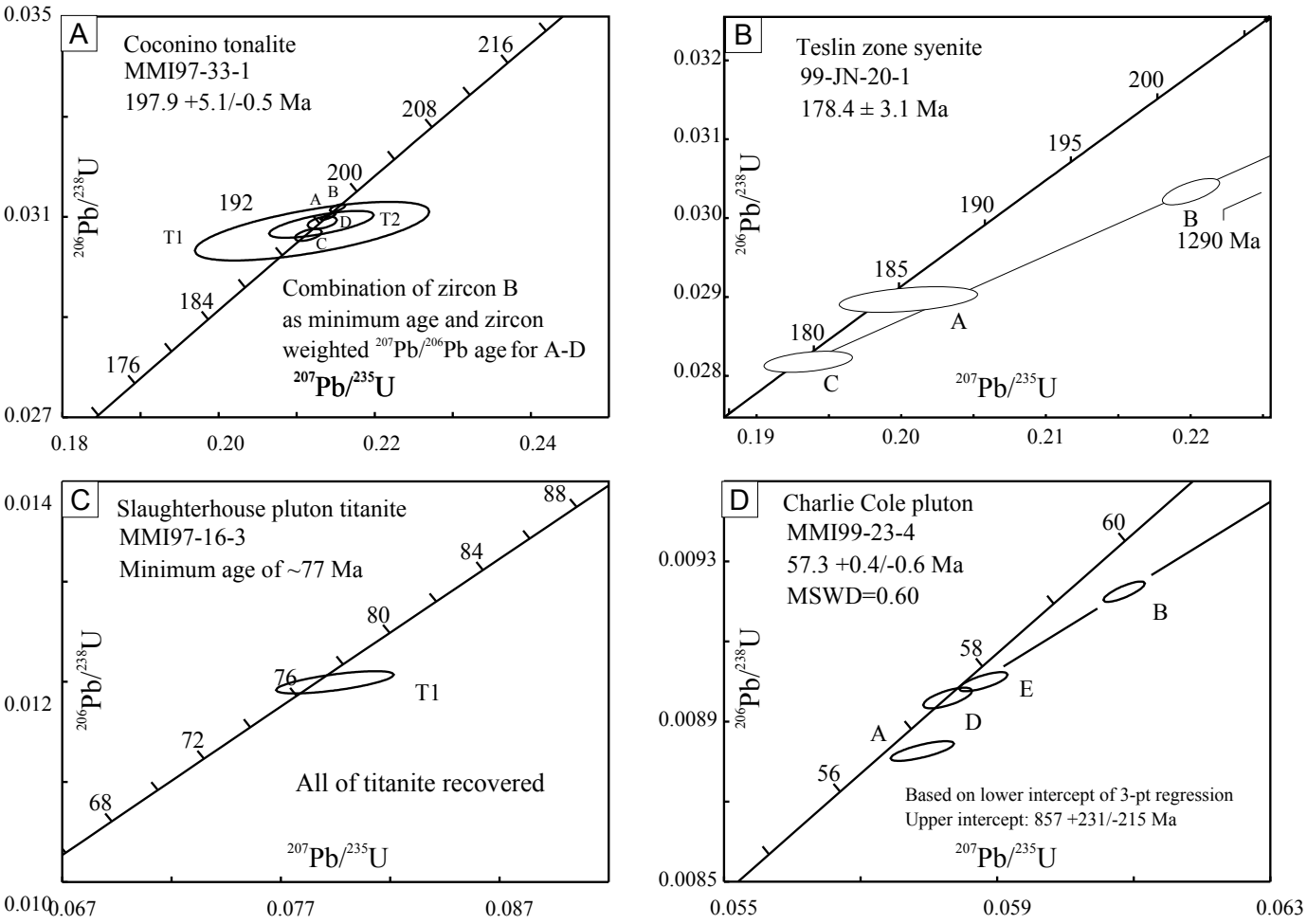

Figure 8. *Concordia plots showing isotopic ratios with error estimates for mineral fractions from Jurassic and younger plutonic rocks: A) Coconino tonalite; B) Teslin zone syenite; C) Slaughterhouse pluton; D) Charlie Cole pluton.*

PAGE PROOFS

multifaceted grains to elongate prisms and thinly tabular to bladed crystals. Titanites are clear, pale yellow fragments of euhedral grains. Results for four strongly abraded zircon fractions are concordant and generally non-overlapping between about 198 Ma and 194 Ma (Fig. 8A; Table 1). The dispersion of data is attributed to minor Pb loss. Elongate prisms of Fraction B gave the oldest result at 197.9 ± 0.5 Ma ($^{206}Pb/^{238}U$ age), which is considered as a minimum crystallization age for the tonalite, as these grains may have experienced minor Pb loss. Combining this minimum age estimate with the more conservative weighted $^{207}Pb/^{206}Pb$ age of 198.1 ± 4.9 Ma for the four analysed zircon fractions leads to an assigned age of 197.9 +5.1/-0.5 Ma. Two concordant and overlapping titanite results at 195.0 ± 3.7 Ma and 195.9 ± 1.7 Ma (T1 and T2, respectively; $^{206}Pb/^{238}U$ ages) record the cooling of the Coconino tonalite through the titanite closure temperature.

Teslin Zone Syenite, 178.4 ± 3.1 Ma (Fig. 8B)

A northwest-elongated pluton and peripheral dike swarms of pink, medium to coarse-grained syenite cut the Big Salmon Complex east of Teslin Lake. A good zircon yield was recovered from a syenite sample collected about 5 km southeast of the mouth of Jennings River (99JN-20-1). The largest zircon population consists of colourless, light tan and tan prisms (1.5 to 2:1 aspect ratio). Some pieces of large tan prisms and broken pieces of colourless needles are also present. All three populations show varying degrees of resorption and clarity. Grains with mineral inclusions and fractures are common. Three zircon fractions were analyzed, including two single broken prismatic grains (fraction A and C) and a small multi-grain (24) population of colourless long prismatic grains (B).

The U-Pb results for these three zircon fractions are presented in Fig. 8B and Table 1. The zircon chemistry as represented by these three fractions is variable, with a range in uranium content (196-764 ppm) and Th/U (0.16-0.51). The two single grain analyses (A and C) overlap within error of the concordia curve and have $^{206}Pb/^{238}U$ ages of 184.1 and 179.1 Ma, respectively. Grain C is the more concordant and precise of the two single grain analyses, and the 179.1 ± 0.6 Ma $^{206}Pb/^{238}U$ age is considered a robust constraint for the age of primary magmatic zircon in the syenite. A reference line constructed to pass through the two more precise analyses (B and C) defines an upper intercept age of *ca.* 1290 Ma and a lower intercept age of 178.4 ± 3.1 Ma. This lower intercept age is controlled by the single grain analysis C and is considered the best estimate for the emplacement age of the Teslin Zone syenite.

Slaughterhouse Titanite (Fig. 8C)

Dark grey to red-weathering quartz diorite underlies southern Teslin Lake (Fig. 2). It is comprised of green, pyroxene-cored hornblende (25%), biotite (10%), titanite (up to 1%), plagioclase (60%) and quartz (10%). Parts of the body are lithologically and petrographically indistinguishable from the Coconino tonalite.

Isotopic age determinations of zircons extracted from two samples collected at localities 7.5 km apart, have been reported previously as 175 Ma (maximum) and 170.7 +5.1/-3.4 (Mihalynuk *et al.*, 2004). Abundant titanite from the first sample yielded 170.9 ± 0.5 Ma, but only a trace of titanite was recovered from the second sample. This small amount of titanite allowed for only one analysis. It is slightly discordant at 77 Ma (Fig. 8C), providing a minimum, but notably younger age than the titanite age previously published, and presumably records the same lead-loss event recorded by the Teslin fault feldspar porphyry (99TF3-2; Appendix 1).

Charlie Cole Pluton, 57.3 +0.4/-0.6 Ma (Fig. 8D)

Strongly foliated, light grey to white-weathering granite underlies Mount Charlie Cole (Gabrielse, 1969), and a few outcrops on its northern flank extend onto the southwestern corner of the map area (Fig. 2). It is medium-grained, consisting of quartz (30%) and plagioclase (30%), with K-feldspar as phenocrysts (20%) and matrix (10%), and 15% smeared, chloritized mafic mineral (biotite?). S-C fabrics are well developed for nearly a kilometre across strike. They indicate sinistral motion on C-planes (Fig. 9).

Zircons are clear, colourless to very pale pink, stubby to very elongate euhedral prisms. Results for four of five analyses appear on concordia plot (Fig. 8D; fraction C is highly discordant and off the plot to right). An age of 57.3 +0.4/-0.6 Ma is based on the lower intercept of a three point York regression. The upper intercept of this chord at *ca.* 860 indicates the average age of inheritance in fractions B and E. Fraction C (Table 1; not plotted) appears to contain older inheritance and/or underwent Pb loss, as did fraction A.

DISCUSSION

Inheritance and lead loss, together with complex metamorphic overgrowths, limits the utility of isotopic age dating of Big Salmon Complex protoliths and intrusions by conventional thermal ionization mass spectroscopic techniques, such as those used in this paper. High resolution ion microprobe analysis of zircon cores and overgrowths is needed to further resolve the metamorphic and structural history of the complex. A lack of suitable protoliths within the oldest rocks of the Big Salmon Complex will continue to thwart attempts at direct age determination; however, additional precise analyses of single detrital zircons will provide increasingly accurate maximum age limit for these rocks.

Within these stated limitations, we correlate depositional and deformational events in the Big Salmon Complex with those known more regionally, and draw tentative conclusions about how the Big Salmon Complex fits into the evolving tectonic framework of the northern Cordillera.

Oldest Big Salmon Complex

The oldest rocks belonging to the Big Salmon Complex are interpreted to be a clastic package including quartz-rich pebble conglomerate and arkosic conglomerate, brown wacke and black slate exposed near the Jennings River. A relative age for this succession is constrained only as older than a cross-cutting dioritic intrusion, which has a reliable U-Pb age determination of 342 ± 2 Ma (MMI99-17-4 *in* Roots *et al.*, 2002). A stratigraphic contact with the presumably overlying Smart River metabasalt has not been observed.

PAGE PROOFS

Attempts to directly date the Smart River metabasalt by extracting zircon or badellyite have been unsuccessful, yielding only abundant apatite and pistacite. A minimum age for the greenstone is based upon an interpreted intrusive contact with the infolded and chilled *ca*. 353 Ma Four Mile Lake tonalite intrusion (Figs. 6B, 7A). An older age constraint may be provided by the Mount Hazel orthogneiss (362.3 +7.9/-6.8 Ma U-Pb; Mihalynuk *et al*., 2000), which is interpreted to cut the greenstone. However, contact relations with the Mount Hazel orthogneiss are equivocal, and an additional age determination of 336.6 ± 0.8 Ma reported here (99JN32-3; Table 1), on a sample of the border phase of the Mount Hazel body, casts doubt on the older interpreted age.

Younging direction, as indicated by geochronological constraints, is consistent with sparse sedimentological evidence, the strongest of which is an unconformity surface overlain by conglomerate. Smart River metabasalt of the Jennings marker succession is older than the 353 Ma intrusions that cuts it, and is probably cut by the Mount Hazel orthogneiss (*ca*. 336 Ma, or possibly *ca*. 362 Ma?). Tuffaceous layers in the heterolithologic unit above the succession have been dated at 325.1 ± 3.0 Ma (Mihalynuk *et al*., 2000; early Late Mississippian, or Serpukhovian, according to the timescale of Okulitch, 2002); an age corroborated by that of a neighbouring tuffaceous bed that yielded an identical age within error (MMI97-35-1b; Table 1).

Direct age determination of the marker succession by paleontological methods has proven similarly problematic. Macrofossil debris do occur within the carbonate unit, but they are silicified and poorly preserved, providing only general age constraints (W. Bamber, written communication, 1998). No microfossils have been recovered from ~10 samples processed.

The Logjam limestone overlying the metachert may be correlative with limestone in the Screw Creek valley to the east (Fig. 2; Stevens and Harms, 1995). Macrofossils recovered from the Screw Creek Limestone give a mid-Mississippian (Viséan) age (W. Bamber, unpublished report, 2000; *ca.* 342-327 Ma; see also Roots *et al*., this volume). Conodonts extracted from interbedded tuff and limestone near the top of the unit in Screw Creek yield a Bashkirian-Moscovian age (*ca.* 314-306 Ma; Orchard, this volume).

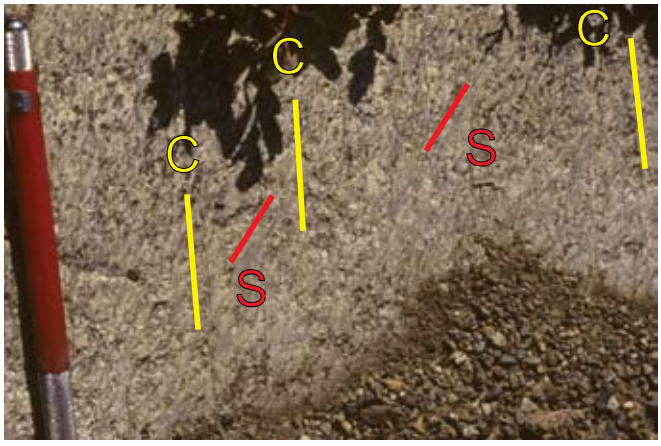

Figure 9. *S-C fabric developed within the Paleocene Charlie Cole pluton.*

Despite the problems with determining the absolute ages of the marker succession protoliths, felsic dikes and tuffaceous units with clear contact relationships have yielded zircons and provide a basis for the structural history presented here. Integration of structural and geochronologic data leads to a five-stage deformational history.

Regional Deformational Events: Ages, Causes and Correlations

Five phases of deformation are outlined by this study; however the earliest, D_i, is cryptic, and the latest, D_4, is a catchall for various late folds and fabrics. Here, we evaluate the regional implications of all of the deformational events recorded in the Big Salmon Complex and speculate on their causes.

D_4

D_4 may not be a distinct deformational event, but probably reflects the combined incremental effects of tectonic exhumation and stress transmitted from large strike slip faults that bound the Big Salmon Complex (*e.g.*, Teslin fault). Both maximum and minimum principal stress orientations, as deduced from D_4 conjugate kink band sets, are consistent with those expected to have formed broad D_4 warps, orogen parallel and orogen normal, as a result of late dextral motion on the Teslin fault (Fig. 5L). Four kilometres south of the inferred trace of the Teslin fault (which strikes N300°), C/S fabrics overprint more than 2 km^2 of the 57.3 +0.4/-0.6 Ma Charlie Cole pluton. Orientation of most of the C-planes is between N185° and N020°, also consistent with orogen-parallel maximum stress (Fig. 5L). Strain partitioning into weak units near the Teslin fault zone is called upon to explain why the 57 Ma Charlie Cole pluton is extensively foliated (Fig. 9) while older plutons a few more kilometres distant are undeformed (*e.g.*, the *ca.* 178 Ma Teslin zone syenite, Fig. 8B). This cautionary example underscores one of the major pitfalls of using the age of "post-kinematic" intrusive rocks to place young limits on the age of deformational events. Furthermore, there is no clear record of the *ca.* 173 Ma collisional event that emplaced Cache Creek blueschist (Mihalynuk *et al*., 2004) immediately outboard of the Big Salmon Complex.

Lead Loss Events

There are currently no reliable isotopic age determinations that directly date deformational events older than the latest regional ductile deformation, D_3. Lead-loss events date D_3 (185 Ma) and perhaps a younger, localized deformation that we collectively attribute to D_4 (77-80 Ma). The widespread 185 Ma lead-loss event (D_3) is coeval with emplacement of the huge Simpson Peak batholith and smaller intrusions of the same age. Samples most strongly affected are the Arsenault dacite (Fig. DR1F) and a nearby tuff in carbonate. Arsenault dacite and adjacent calcareous tuff both host skarn-style mineralization at the Arsenault prospect. This mineralization is probably related to Early Jurassic plutonic rocks in the subsurface. Lead isotope model ages from chalcopyrite fall within a Middle

PAGE PROOFS

Triassic to Middle Jurassic cluster (Mortensen and Gabites, 2002). Epidote-altered quartz-feldspar porphyritic dikes intersected by exploration drilling on the property are probably offshoots from a mass of Simpson Peak batholith in the subsurface.

The younger, 77-80 Ma lead loss event appears to be restricted to units within 5 km of the Teslin fault, including a dioritic sill within 100 m of the exposed trace of the fault. Titanite from samples of the Middle Jurassic Slaughterhouse pluton collected near the Teslin fault show lead loss; those collected away from the fault do not. Localized Pb-loss may be related to hydrothermal fluid flow focused near the Teslin fault.

D_3

In style, scale, degree of fabric transposition and possible age, the folds produced by D_3 are similar to F_3 reported by de Keijzer *et al.* (1999) in the Teslin zone, including the regional-scale, east-vergent Grizzly synform. These authors provide no precise age constraints on the deformational event that gave rise to F_3, but state that it probably post-dated *ca.* 239 Ma muscovite cooling ages obtained from the *ca.* 269 Ma (U-Pb zircon; Creaser *et al.*, 1997) Last Peak eclogite, and was of sufficiently low metamorphic grade to avoid resetting the muscovite.

High-amplitude, northeast-verging F_3 folds involved Triassic conodont-bearing, black shale of the Teh formation in the Nasty Peak area (Fig. 2; see also Roots *et al.*, this volume), placing a maximum age constraint on D_3. Youngest regional ductile fabrics are cut by the Early Jurassic Simpson Peak batholith (K-Ar hornblende is 185 ± 14 Ma, recalculated from Wanless *et al.*, 1970), undeformed Early Jurassic dikes (Nelson and Friedman, 2004), and the undeformed 178.4 ± 3.1 Ma Teslin Zone syenite (Fig. 8B), providing a minimum age constraint of *ca.* 185 Ma. The oldest phases of the Simpson Peak batholith locally display a weak tectonic foliation. Younger phases are undeformed, cut the older phases and, based on extrapolated contacts, are also interpreted to cut the 197.9 +5.1/-0.5 Ma Coconino tonalite (Figs. 2, 7A) and its strong D_3 fabric. D_3 deformation appears to have been a short pulse at *ca.* 185 Ma, assuming that the foliated phases of the Simpson Peak batholith are nearly coeval with non-foliated phases. Evidence of deformation of this age is widespread in southwest Yukon and adjacent parts of Alaska and British Columbia. Cooling ages reported by Gordey *et al.* (1998), from hornblende and biotite in greenstone along strike to the northwest, are 183.6 ± 2 and 187.4 ± 5.2 Ma. We interpret the widespread lead-loss event at 185-190 Ma as dating the D_3 event.

An intense orogenic pulse was recorded in the northern Canadian Cordillera at *ca.* 186 Ma, probably related to initial emplacement of Quesnellia onto pericratonic strata at between 186 and 181 Ma (Nixon *et al.*, 1993), with a synchronous shift towards more evolved Nd isotopic signatures in both igneous bodies and sedimentary strata (Erdmer *et al.*, 2005; Petersen *et al.* 2004). It is both coeval with, and of the same short duration as, extremely rapid uplift recorded by the c*a.* 186 Ma mid-crustal Aishihik plutonic suite of southeast Yukon, which is cut by plutons of the Long Lake suite that intruded at shallow depths. Isotopic ages of the Aishihik and Long Lake suites are indistinguishable (Johnston and Erdmer, 1995). In northwestern B.C., intrusive events correlated with the Aishihik and Long Lake suites indicate intrusion and rapid uplift are within 6 Ma (Mihalynuk *et al.*, 1999), and farther south along strike, a profound, sub-185 Ma unconformity has been well constrained by Brown *et al.* (1996). In eastern Alaska, a broad area of Yukon-Tanana rocks display cooling ages between 185 and 188 Ma (Dusel-Bacon *et al.*, 2002; Hansen *et al.*, 1991).

Stevens *et al.* (1993) reported a U-Pb zircon age for a post-deformational quartz diorite pluton in the Teslin zone of 188.0 +2.7/-5.4 Ma (minimum age of 182.6 Ma), and $^{40}Ar/^{39}Ar$ cooling ages from the same body of 182 ± 2 Ma (hornblende) and 179 ± 2 Ma (biotite). These cooling ages are younger than white mica cooling ages from samples collected about 60 km farther northwest along the Teslin zone (Hansen *et al.*, 1991), which cluster in the range of 191 to 196 Ma.

Most reliable magmatic and cooling ages point to a widespread deformational and cooling event in southwest Yukon and adjacent parts of Alaska and British Columbia between *ca.* 191 and *ca.* 181 Ma. A swarm of orogen-parallel granodiorite dykes and tabular stocks, which intruded the east flank of the Big Salmon Complex around 185 Ma (Nelson and Friedman, 2004, fig. 2), may show that the region experienced local, orogen-normal extension by 185 Ma.

D_2

D_2 is a deformational event to which the younger of two early transposition fabrics, S_2, is attributed. S_2 is imposed on a 330.7 +8.8/-5.4 Ma dike, which cuts the oldest fabric, S_1, attributed to D_1. It also folds the heterogeneous clastic unit, including the 325 ± 3 Ma dacite tuff unit. D_2 is therefore constrained as younger than *ca.* 340 Ma (the dike age at the oldest limit of error, and than *ca.* 328 Ma, which is the oldest age of the dacite tuff); and older than *ca.* 197 Ma (the cross-cutting Coconino tonalite at the youngest limit of error). No further refinement can reliably be made based upon the age data available, and because the widespread lead-loss event is expected to have reset any older cooling ages, we have not attempted to extract an older cooling age history from the metamorphic minerals.

We tentatively correlate D_2 fabrics with S_2 of de Keijzer *et al.* (1999); both are the younger of two transposition fabrics. These authors attribute S_2 to a fold event during obduction of rock units within the Grizzly synform (which includes most of the Teslin zone) over the continental margin. In this interpretation, the principal enveloping surface of the Grizzly synform is a suture along which eclogite-bearing Last Peak klippe was emplaced. Assuming that the muscovite cooling age and peak metamorphic U-Pb ages of the Last Peak eclogite are correctly interpreted (Creaser *et al.* 1997), the continent-ward obduction event took place between *ca.* 269 and *ca.* 239 Ma.

Kinematics of D_2 in the Big Salmon Complex have not been resolved. General eastward closure of mountain-scale F_2 folds that form the enveloping surface of the Smart River metabasalt, for example along the western flank of Mount Francis, are consistent with their formation during continent-ward emplacement, but they are not reliable kinematic indicators.

A D_2 age of *ca.* 270 Ma has been suggested (Mihalynuk *et al.*, 2000), coeval with Middle Permian cooling ages in eclogite and

PAGE PROOFS

blueschist along strike to the north (Erdmer *et al*., 1998). If correlation between D_2 and Teslin zone S_2 fabrics is correct, a 270 Ma D_2 would now appear to be, at a minimum, 10 Ma too old. Precise geochronological age determinations reveal a *ca*. 259 peak metamorphic event in western Yukon (Villeneuve *et al*., 2003). A lack of precise timing for D_2 in the Big Salmon Complex precludes definite correlation with regional deformational events, and a local event cannot be ruled out. Nevertheless, we suggest that D_2 correlates with the Late Permian deformational event at *ca*. 260 Ma, as part of a regional event supported by a growing body of evidence.

D_1

The oldest regional deformation, D_1, is younger than the oldest phase of the Mount Hazel orthogneiss and Four Mile tonalite (362.2 +7.9/-6.8 and 352.9 ± 1.4 Ma, respectively), which both appear to have been affected by all phases of subsequent regional deformation, together with adjacent country rocks. Minimum limits on the age of D_1 are provided by the post-D_1 dike (330.7 +8.8/-5.4 Ma), and possibly by the Jennings Knee porphyry (336 +16/-1 Ma), which is interpreted to cut stratigraphy younger than the conglomerate attributed to D_1.

Relationships are less certain, but D_1 also appears to be younger than the Mount Francis quartz-feldspar porphyry (*ca*. 340 Ma), because clasts of the porphyry are interpreted as included in a conglomerate unit attributed to post-D_1 erosion. Deposition of Logjam limestone was interrupted by an erosional event, in several places marked by coarse polymictic conglomerate tens of metres thick. Near Mount Francis, this erosional surface has cut down into the Smart River metabasalt (Fig. 2), clearly an angular unconformity with significant relief. However, preserved D_1 fabrics formed at a depth where greenschist-facies minerals were stable, not at the surface as indicated by the conglomerate.

D_1 is thus bracketted conservatively between *ca*. 353 Ma and *ca*. 331 Ma, or between *ca*. 340 Ma and *ca*. 331 Ma if it corresponds to the sub-Logjam limestone unconformity. Stevens *et al*. (1996) infer similar timing for early deformational fabrics in the Teslin zone, which overprint Early Mississippian tonalite, probably belonging to the Mount Hazel suite. The age of early transposition fabrics mapped by de Keijzer *et al*. (1999) is similarly constrained.

D_1 could be coeval with a deformational event reported by Colpron *et al*. (this volume-b), which is constrained on the basis of deformed and cross-cutting undeformed plutons as *ca*. 340-344 Ma. It also would be roughly coeval with the deformational event indicated by conglomerate at the base of the Screw Creek Limestone (Roots *et al*., this volume).

Cryptic Event D_i

Fabrics associated with D_i, preserved as a schistosity outlined by inclusion trails within porphyroblasts (S_i), may be controlled by a number of factors. For example, protoliths may have required a sufficiently high argillaceous component to produce the early schistosity, bulk rock composition needed to be suitable for porphyroblast growth, or retrograde conditions were muted enough to permit preservation of porphyroblasts containing S_i. It is possible that coeval structures are present in Big Salmon Complex suprastructure, but are not recognized due to lower pressure and temperature conditions and consequent lack of porphyroblast development at such high structural levels. Alternatively, the fabrics may be due to amphibolite facies metamorphism at or before 362.3 +7.9/-6.8 Ma (because the Mount Hazel orthogneiss, interpreted to be this age, is overprinted by all succeeding fabrics).

Clear evidence of a 362 Ma or older deformational event is lacking within the northern Cordillera. Yet a Late Devonian (mid-Frasnian) to Early Mississippian (mid-Osagian) deformation is well documented in the Roberts Mountains allochthon in Nevada (Johnson and Pendergast, 1981) and hints of such an event extend along the Cordillera to the Yukon according to Smith *et al*. (1993) and Root (2001). Much evidence points to the opening of the Slide Mountain basin at this time, as a back-arc basin (*e.g*., Ferri, 1997) *via* slab roll-back, but could continental-scale deformation result from this mechanism? The viability of back-arc basin initiation and growth by slab roll-back has been questioned by some authors (*e.g*., Mantovani *et al*., 2001), who suggest that the initiators of back-arc spreading are collisions in either the upper or lower plates that lead to escape in the upper plate. Others, such as Nishimura (2002), and Maruyama and Liou (2003) point to the current development of back-arc basins only in the western Pacific and attribute their distribution to subduction of old, hydrated crust and consequent elevation of H_2O, decrease in both viscosity and strength, and increase rate of convection of the overlying mantle wedge.

In the case of the best developed back-arc basin in the circum-Pacific region, the Japan Sea, deformation and widespread mafic volcanism (over 50,000 km^2) of outer China accompanied the early stages of spreading (Liu *et al*., 2001). In an analogous sense, mafic volcanic rocks are common within the pericratonic strata of the Yukon-Tanana terrane and in inboard shelf to slope strata. Some intermediate to mafic volcanism is of the appropriate age and composition (*e.g*., Fig. 1; see compilation and discussion in Erdmer *et al*., 2005), but most is of unknown age due to the problems of dating such successions using isotopic methods, as is demonstrated by the Smart River metabasalt. We speculate that, as in the case of the Japan Sea, initiation of the Slide Mountain back-arc basin was accompanied by regional deformation, and that this produced the early cryptic fabric recorded by the Big Salmon Complex. Testing such a hypothesis might involve microanalytical isotopic evaluation of titanite inclusions in early poikiloblasts to reveal the age of the early deformational event. Conclusive linkage with opening of the Slide Mountain basin will require further regional structural and stratigraphic work.

SUMMARY

Greenschist and relict amphibolite facies arc and quartz-rich sedimentary rocks of the Big Salmon Complex are part of the Yukon-Tanana terrane, a Devonian to Triassic arc complex which includes deformed equivalents of the Quesnel arc. The oldest volcano-sedimentary parts of the complex have been deformed in at least four events. Folds attributable to various events can be traced regionally where outlined by a persistent, four-unit marker succession, the

PAGE PROOFS

Jennings marker. Approximate ages of the stratigraphy and deformational events are interpreted from thermal ionization mass spectroscopic analysis of zircon and titanite extracted from tuffaceous rocks and variably deformed intrusions within the complex. The youngest pervasive fabrics formed during D_3 emplacement of Quesnellia, which is a regional thermal and lead-loss event that masks the age of older units and deformational events, D_2 and D_1.

D_2 is loosely constrained as between *ca.* 325 and *ca.* 198 Ma. It may be attributed to a *ca.* 260 Ma event that is well developed regionally in the Yukon-Tanana terrane. D_1 is constrained as between 353 and 331 Ma, perhaps *ca.* 340-344 Ma, synchronous with a deformational event outlined in Yukon.

Cryptic evidence of a potentially older deformational event, D_i, is preserved only as inclusion trails in porphyroblasts. The youngest "event", D_4, is poorly defined, but may be related to motion on crustal-scale faults that bound the Big Salmon Complex. Ductile fabrics attributed to D_4 are developed in plutons as young as 57 Ma, but do not affect country rocks regionally. Distribution of D_4 fabrics is presumably due to the partitioning of strain into thermally weakened plutonic rocks and surrounding aureoles.

ACKNOWLEDGMENTS

Field and laboratory studies were supported by the Ancient Pacific Margin NATMAP (National Mapping Program), the B.C. Ministry of Energy and Mines, and the University of British Columbia (Friedman). Geochronological facilities at UBC and U of A are supported by NSERC Discovery grants to Mortensen and Heaman, respectively. Comments by C. Roots and M. Colpron improved an earlier version of the manuscript, and a thorough review by V. McNicoll was very helpful. Volume editors M. Colpron and J. Nelson made numerous copy edits to improve text and figure legibility.

REFERENCES

Brown, D.A., Gunning, M.H. and Greig, C.J., 1996, The Stikine Project: Geology of western Telegraph Creek map area, northwestern British Columbia (NTS 104G/5, 6, 11W, 12 and 13): B.C. Ministry of Employment and Investment, Geological Survey Branch, Bulletin 95, 175 p.

Colpron, M., Nelson, J.L. and Murphy, D.C., this volume-a, A tectonostratigraphic framework for the pericratonic terranes of the northern Cordillera, *in* Colpron, M. and Nelson, J.L., eds., Paleozoic Evolution and Metallogeny of Pericratonic Terranes at the Ancient Pacific Margin of North America, Canadian and Alaskan Cordillera: Geological Association of Canada, Special Paper 45, p. ???.

Colpron, M., Mortensen, J.K., Gehrels, G.E. and Villeneuve, M.E., this volume-b, Basement complex, Carboniferous magmatism and Paleozoic deformation in Yukon-Tanana terrane of central Yukon: Field, geochemical and geochronological constraints from Glenlyon map area, *in* Colpron, M. and Nelson, J.L., eds., Paleozoic Evolution and Metallogeny of Pericratonic Terranes at the Ancient Pacific Margin of North America, Canadian and Alaskan Cordillera: Geological Association of Canada, Special Paper 45, p. ???.

Creaser, R.A., Erdmer, P., Grant, S.L. and Stevens, R.A., 1995, Tectonic identity of Teslin tectonic zone metasedimentary strata; Nd isotopic and geochemical constraints [abstract]: Geological Association of Canada, Program with Abstracts, v. 20, p. 21.

Creaser, R.A., Heaman, L.M. and Erdmer, P., 1997, Timing of high-pressure metamorphism in the Yukon-Tanana Terrane, Canadian Cordillera; constraints from U-Pb zircon dating of eclogite from the Teslin tectonic zone: Canadian Journal of Earth Sciences, v. 34, p. 709-715.

de Keijzer, M., Mihalynuk, M.G. and Johnston, S.T., 2000, Structural investigation of an exposure of the Teslin Fault, northwestern British Columbia: Geological Survey of Canada, Paper 2000-A5, 10 p.

de Keijzer, M. and Williams, P.F., 1997, A new view on the structural framework of the Teslin Zone, south-central Yukon [abstract], *in* Cook, F.A. and Erdmer, P., eds., Lithoprobe Slave-Northern Cordillera Lithospheric Evolution (SNORCLE) and Cordilleran Tectonics Workshop: Lithoprobe Report No. 56, p. 96-102.

de Keijzer, M., Williams, P.F. and Brown, R.L., 1999, Kilometre-scale folding in the Teslin Zone, northern Canadian Cordillera, and its tectonic implications for the accretion of the Yukon-Tanana Terrane to North America: Canadian Journal of Earth Sciences, v. 36, p. 479-494.

Dusel-Bacon, C., Lanphere, M.A., Sharp, W.D., Layer, P.W. and Hansen, V.L., 2002, Mesozoic thermal history and timing of structural events for the Yukon-Tanana Upland, east-central Alaska: $^{40}Ar/^{39}Ar$ data from metamorphic and plutonic rocks: Canadian Journal of Earth Sciences, v. 39, p. 1013-1051.

Erdmer, P., 1985, An examination of the cataclastic fabrics and structures of parts of Nisutlin, Anvil and Simpson allochthons, central Yukon; test of the arc-continent collision model: Journal of Structural Geology, v. 7, p. 57-72.

Erdmer, P., Ghent, E.D., Archibald, D.A. and Stout, M.Z., 1998, Paleozoic and Mesozoic high-pressure metamorphism at the margin of ancestral North America in central Yukon: Geological Society of America Bulletin, v. 110, p. 615-629.

Erdmer, P. and Helmstaedt, H., 1983, Eclogite from central Yukon: a record of subduction at the western margin of ancient North America: Canadian Journal of Earth Sciences, v. 20, p. 1389-1408.

Erdmer, P., Mihalynuk, M.G., Gabrielse, H., Heaman, L.M. and Creaser, R.A., 2005, Mississippian volcanic assemblage conformably overlying Cordilleran miogeoclinal strata, Turnagain River area, northern British Columbia, is not part of an accreted terrane: Canadian Journal of Earth Sciences, v. 42, p. 1449-1465.

Ferri, F., 1997, Nina Creek Group and Lay Range assemblage, north-central British Columbia: remnants of late Paleozoic oceanic and arc terranes: Canadian Journal of Earth Sciences, v. 34, p. 854-874.

Foster, H.L., Keith, T.E.C. and Menzie, W.D., 1994, Geology of the Yukon-Tanana area of east-central Alaska (Chapter 6), *in* Plafker, G. and Berg, H. C., eds., The Geology of Alaska: Geological Society of America, The Geology of North America, v. G-1, p. 205-240.

Friedman, R.M., Diakow, L.J., Lane, R.A., and Mortensen, J.K., 2001, U–Pb age constraints on latest Cretaceous magmatism and associated mineralization in the Fawnie Range, Nechako Plateau, central British Columbia: Canadian Journal of Earth Sciences, v. 38, p. 619-637.

Gabrielse, H., 1969, Geology of Jennings River map-area: Geological Survey of Canada, Paper 68-55, 37 p.

Gordey, S.P., 1992, Geological fieldwork in Teslin map-area, southern Yukon Territory: Geological Survey of Canada, Paper 92A, p. 279-286.

Gordey, S.P. and Stevens, R.A., 1994, Geology, Teslin, Yukon Territory: Geological Survey of Canada, Open File 2886, 1:250,000.

Gordey, S.P., McNicoll, V.J. and Mortensen, J.K., 1998, New U-Pb ages from the Teslin area, southern Yukon, and their bearing on terrane evolution in the northern Cordillera, *in* Radiogenic age and isotopic studies: Geological Survey of Canada, Report 11, p. 129-148.

Hansen, V.L., 1989, Structural and kinematic evolution of the Teslin suture zone, Yukon; record of an ancient transpressional margin: Journal of Structural Geology, v. 11, p. 717-733.

Hansen, V.L., 1992a, Backflow and margin-parallel shear within an ancient subduction complex: Geology, v. 20, p. 71-74.

Hansen, V.L., 1992b, P-T evolution of the Teslin suture zone and Cassiar tectonites, Yukon, Canada; evidence for A- and B-type subduction: Journal of Metamorphic Geology, v. 10, p. 239-263.

Hansen, V.L., Heizler, M.T. and Harrison, T.M., 1991, Mesozoic thermal evolution of the Yukon-Tanana composite terrane; new evidence from $^{40}Ar/^{39}Ar$ data: Tectonics, v. 10, p. 51-76.

PAGE PROOFS

Hansen, V.L., Mortensen, J.K. and Armstrong, R.L., 1989, U-Pb, Rb-Sr, and K-Ar isotopic constraints for ductile deformation and related metamorphism in the Teslin suture zone, Yukon-Tanana terrane, south-central Yukon: Canadian Journal of Earth Sciences, v. 26, p. 2224-2235.

Heaman, L.M., Erdmer, P., and Owen, J.V., 2002. U-Pb geochronologic constraints on the crustal evolution of the Long Range inlier, Newfoundland: Canadian Journal of Earth Sciences, v. 39, p. 845-865.

Johnson, J.G. and Pendergast, A., 1981, Timing and mode of emplacement of the Roberts Mountains allochthon, Antler orogeny: Geological Society of America Bulletin, v. 92, p. 648-658.

Johnston, S.T. and Erdmer, P., 1995, Magmatic flow and emplacement foliations in the Early Jurassic Aishihik batholith, Southwest Yukon; implications for northern Stikinia, *in* Miller, D.M. and Busby, C., eds., Jurassic Magmatism and Tectonics of the North American Cordillera: Geological Society of America, Special Paper 299, p. 65-82.

Krogh, T.E., 1982, Improved accuracy of U-Pb ages by the creation of more concordant systems using an air abrasion technique: Geochimica et Cosmochimica Acta, v. 46, p. 637-649.

Liu, J., Han, J. and Fyfe, W.S., 2001, Cenozoic episodic volcanism and continental rifting in northeast China and possible link to Japan Sea development as revealed from K-Ar geochronology: Tectonophysics, v. 339, p. 385-401.

Ludwig, K.R., 1980, Calculation of uncertainties of U-Pb isotope data: Earth and Planetary Science Letters, v. 46, p. 212-220.

Mattinson, J.M. 1994, A study of complex discordance in zircons using step-wise dissolution techniques: Contributions to Mineralogy and Petrology, v. 116, 117–129.

Mantovani, E., Viti, M., Babbucci, D., Tamburelli, C. and Albarello, D., 2001, Back-arc extension: which driving mechanism?: Journal of the Virtual Explorer, v. 3, p. 17-45.

Maruyama, S. and Liou, J.G., 2003, The western Pacific triangular zone: frontier to form a future supercontinent [abstract]: Geological Society of America, Abstracts with Programs, v. 35, no. 6, p. 428.

Mihalynuk, M.G. and Peter, J.M., 2001, A hydrothermal origin for "crinkle chert" of the Big Salmon Complex: B.C. Ministry of Energy and Mines, Paper 2001-1, p. 83-84.

Mihalynuk, M.G., Nelson, J.L. and Friedman, R.M., 1998, Regional geology and mineralization of the Big Salmon Complex (104N NE and 1040 NW): B.C. Ministry of Energy and Mines, Paper 1998-1, p. 6.1-6.20.

Mihalynuk, M.G., Mountjoy, K.J., Smith, M.T., Currie, L.D., Gabites, J.E., Tipper, H.W., Orchard, M.J., Poulton, T.P. and Cordey, F., 1999, Geology and mineral resources of the Tagish Lake area (NTS 104M/ 8,9,10E, 15 and 104N/ 12W), northwestern British Columbia: B.C. Ministry of Energy and Mines, Bulletin 104, 217 p.

Mihalynuk, M.G., Nelson, J.L., Gleeson, T.P., Roots, C.F., and de Keijzer, M., 2000a, Geology of Smart River (NTS 104O/13): B.C. Ministry of Energy and Mines, Open File 2000-6, 1:50,000.

Mihalynuk, M.G., Nelson, J.L., Roots, C.F., Friedman, R.M. and de Keijzer, M., 2000b, Ancient Pacific Margin Part III: Regional geology and mineralization of the Big Salmon Complex (NTS 104N/9E, 16 & 104O/12, 13, 14W): B.C. Ministry of Energy and Mines, Paper 2000-1, p. 27-46.

Mihalynuk, M.G., Harms, T.A., Roots, C.F., Nelson, J.L., de Keijzer, M., Friedman, R.M. and Gleeson, T.P., 2001a, Geology of Teh Creek (NTS 104N/12): B.C. Ministry of Energy and Mines, Open File 2001-17, 1:50,000.

Mihalynuk, M.G., Nelson, J.L., Friedman, R.M., Gleeson, T.P. and Roots, C.F., 2001b, Geology of Gladys River (NTS 104N/16): B.C. Ministry of Energy and Mines, Open File 2001-4, 1:50,000.

Mihalynuk, M., Erdmer, P., Ghent, E.D., Cordey, F., Archibald, D.A., Friedman, R.M. and Johannson, G.G., 2004, Coherent French Range blueschist: Subduction to exhumation in <2.5 m.y.?: Geological Society of America Bulletin, v. 116, p. 910-922.

Mortensen, J.K., 1992, Pre-mid-Mesozoic tectonic evolution of the Yukon-Tanana Terrane, Yukon and Alaska: Tectonics, v. 11, p. 836-853.

Mortensen, J.K. and Gabites, J.E., 2002, Lead isotopic constraints on the metallogeny of southern Wolf Lake, southeastern Teslin and northern Jennings River map areas, Yukon and British Columbia: preliminary results, *in* Emond, D.S., Weston, L.H. and Lewis, L.L., eds., Yukon Exploration and Geology 2001: Exploration and Geological Services Division, Yukon Region, Indian and Northern Affairs Canada, p. 179-188.

Mulligan, R., 1963, Geology of Teslin map-area, Yukon Territory (105C): Geological Survey of Canada, Memoir 326, 96 p.

Nelson, J.L. and Friedman, R.M., 2004, Superimposed Quesnel (late Paleozoic-Jurassic) and Yukon-Tanana (Devonian-Mississippian) arc assemblages, Cassiar Mountains, northern British Columbia: Field, U-Pb and igneous petrochemical evidence: Canadian Journal of Earth Sciences, v. 41, p. 1201-1235.

Nishimura, S., 2002, Why are there no back-arc basins around the eastern Pacific margin?: Revista Mexicana de Ciencias Geologicas, v. 19, p. 170-174.

Nixon, G.T., Archibald, D.A. and Heaman, L.M., 1993, $^{40}Ar/^{39}Ar$ and U-Pb geochronometry of the Polaris Alaskan-type complex, British Columbia; precise timing of Quesnellia-North America interaction [abstract]: Geological Association of Canada, Program with Abstracts, v. 18, p. 76.

Okulitch, A.V., 2002, Geological time chart, 2002: Geological Survey of Canada, Open File 3040, National Earth Science Series, Geological Atlas - REVISION.

Orchard, M.J., this volume, Late Paleozoic and Triassic conodont faunas of Yukon Territory and northern British Columbia and implications for the evolution of the Yukon-Tanana terrane, *in* Colpron, M. and Nelson, J.L., eds., Paleozoic Evolution and Metallogeny of Pericratonic Terranes at the Ancient Pacific Margin of North America, Canadian and Alaskan Cordillera: Geological Association of Canada, Special Paper 45, p. ???.

Parrish, R.R., Roddick, J.C., Loveridge, W.D. and Sullivan, R.W., 1987, Uranium-lead analytical techniques at the Geochronology Laboratory, Geological Survey of Canada: Geological Survey of Canada, Paper 87-2, p. 3-7.

Petersen, N., Smith, P.L., Mortensen, J.K., Creaser, R.A. and Tipper, H.W., 2004, Provenance of Jurassic sedimentary rocks of south-central Quesnellia, British Columbia: implications for paleogeography: Canadian Journal of Earth Sciences, v. 41, p. 103-125.

Piercey, S.J., Nelson, J.L., Colpron, M., Dusel-Bacon, C., Roots, C.F. and Simard, R.-L., this volume, Paleozoic magmatism and crustal recycling along the ancient Pacific margin of North America, northern Cordillera, *in* Colpron, M. and Nelson, J.L., eds., Paleozoic Evolution and Metallogeny of Pericratonic Terranes at the Ancient Pacific Margin of North America, Canadian and Alaskan Cordillera: Geological Association of Canada, Special Paper 45, p. ???.

Poliquin, M., 2004, Drilling encounters new VMS Cu-Zn-Au-Ag-Pb system at the Mor prospect, Yukon: Almaden Minerals Ltd., Press release, October 29, 2004.

Roddick, J.C., 1987, Generalized numerical error analysis with applications to geochronology and thermodynamics: Geochimica et Cosmochimica Acta, v. 51, p. 2129-2135.

Root, K.G., 2001, Devonian Antler fold and thrust belt and foreland basin development in the southern Canadian Cordillera: implications for the Western Canada Sedimentary Basin: Bulletin of Canadian Petroleum Geology, v. 49, p. 7-36.

Roots, C.F. and Heaman, L.M., 2001, Mississippian U-Pb dates from Dorsey terrane assemblages in the upper Swift River area, southern Yukon Territory: Geological Survey of Canada, Paper 2001-A1, 16 p.

Roots, C.F., Harms, T.A., Simard, R.-L., Orchard, M.J. and Heaman, L.M., 2002, Constraints on the age of the Klinkit assemblage east of Teslin Lake, northern British Columbia: Geological Survey of Canada, Paper 2002-A7, 11 p.

Roots, C.F., Nelson, J.L., Simard, R.-L. and Harms, T.A., this volume, Continental fragments, mid-Paleozoic arcs and overlapping late Paleozoic arc and Triassic sedimentary strata in the Yukon-Tanana terrane of northern British Columbia and southern Yukon, *in* Colpron, M. and Nelson, J.L., eds., Paleozoic Evolution and Metallogeny of Pericratonic Terranes at the Ancient Pacific Margin of North America, Canadian and Alaskan Cordillera: Geological Association of Canada, Special Paper 45, p. ???.

Silberling, N.J., Jones, D.L., Monger, J.W.H. and Coney, P.J., 1992, Lithotectonic terrane map of the North American Cordillera: U.S. Geological Survey, Miscellaneous Investigation Map I-2176, 1:5,000,000.

Smith, M.T., Dickinson, W.R. and Gehrels, G.E., 1993, Contractional nature of Devonian-Mississippian Antler tectonism along the North American continental margin: Geology, v. 21, p. 21-24.

Stevens, R.A., 1992, Regional geology, fabric, and structure of the Teslin suture zone in northwest Teslin map area, Yukon Territory: Geological Survey of Canada, Paper 92A, p. 287-295.

Stevens, R.A. and Erdmer, P., 1993, Tectonic evolution of the Teslin suture zone, south-central Yukon Territory; subduction, transpression and extrusion [abstract]: Geological Association of Canada, Program with Abstracts, v. 18, p. 100.

PAGE PROOFS

Stevens, R.A. and Harms, T.A., 1995a, Investigations in the Dorsey terrane; Part 1, Stratigraphy, structure, and metamorphism in the Dorsey Range, southern Yukon Territory and northern British Columbia: Geological Survey of Canada, Paper 96-1A, p. 117-127.

Stevens, R.A. and Harms, T.A., 1995b, Stratigraphy, structure and metamorphism in the Dorsey Range, southern Yukon Territory and northern British Columbia, *in* Cook, F.A. and Erdmer, P., eds., Slave-Northern Cordillera Lithospheric Evolution (SNORCLE) and Cordilleran Tectonics Workshop: Lithoprobe Report No. 44, p. 69-87.

Stevens, R.A., Mortensen, J.K. and Hunt, P.A., 1993, U-Pb and $^{40}Ar/^{39}Ar$ geochronology of plutonic rocks from the Teslin suture zone, Yukon Territory: Geological Survey of Canada, Paper 93-2, p. 83-90.

Stevens, R.A., Erdmer, P., Creaser, R.A. and Grant, S.L., 1996, Mississippian assembly of the Nisutlin assemblage; evidence from primary contact relationships and Mississippian magmatism in the Teslin tectonic zone, part of the Yukon-Tanana Terrane of south-central Yukon: Canadian Journal of Earth Sciences, v. 33, p. 103-116.

Tempelman-Kluit, D.J., 1979, Transported cataclasite, ophiolite and granodiorite in Yukon; evidence of arc-continent collision: Geological Survey of Canada, Paper 79-14, 27 p.

Thirlwall, M.F., 2000, Inter-laboratory and other errors in Pb isotope analyses investigated using a ^{207}Pb-^{204}Pb double spike: Chemical Geology, v. 163, p. 299-322.

Villeneuve, M.E., Ryan, J.J., Gordey, S.P. and Piercey, S.J., 2003, Detailed thermal and provenance history of the Stewart River area (Yukon-Tanana Terrane, western Yukon) through application of SHRIMP, Ar-Ar and TIMS [abstract]: Geological Association of Canada - Mineralogical Association of Canada - Society of Economic Geologists Abstracts, v. 28, Abstract 344.

Wanless, R.K., Stevens, R.D., Lachance, G.R. and Delabio, R.N., 1970, Age determinations and geological studies - K-Ar isotopic ages: Geological Survey of Canada, Report 9, 78 p.

Wheeler, J.O. and McFeely, P., 1991, Tectonic assemblage map of the Canadian Cordillera and adjacent parts of the United States of America: Geological Survey of Canada, Map 1712A, 1:2,000,000.

Wheeler, J.O., Brookfield, A.J., Gabrielse, H., Monger, J.W.H., Tipper, H.W., and Woodsworth, G.J., 1991, Terrane map of the Canadian Cordillera: Geological Survey of Canada, Map 1713A, 1:2,000,000.

PAGE PROOFS